Alonso, E. E. *et al.* (2011). *Géotechnique* **61**, No. 5, 387–407 [**doi:** 10.1680/geot.SIP11.P.013]

Modelling the response of Lechago earth and rockfill dam

E. E. ALONSO*, S. OLIVELLA*, A. SORIANO†, N. M. PINYOL* and F. ESTEBAN‡

Lechago dam (Teruel, Spain) is a 40 m high zoned earth and rockfill dam sitting on soft continental deltaic deposits. A relatively narrow central clay core is stabilised by wide rockfill shoulders. The dam was well instrumented and continuous records of stress development, pore-water pressures and vertical displacements are available for the construction period. Compaction conditions were followed by means of laboratory and in situ control tests. Core clay material was investigated by means of tests performed on compacted specimens of tertiary clays. Rockfill samples were excavated in outcrops of highly fractured Cambrian quartzitic shale. A testing programme on compacted rockfill gravels was conducted under relative humidity control in a large-diameter oedometer and triaxial cells. A coupled finite-element model has been developed to analyse the tests performed and dam behaviour during construction. Model predictions, essentially based on laboratory tests, are compared with measurements during construction. The predicted response of the dam under an assumed programme of impounding is also given. In the future, once impounding occurs, it will be possible to compare these predictions with actual dam performance. The paper provides an integrated description of the dam design, construction and early behaviour. It presents a procedure to interpret available data (laboratory as well as in situ data) on compacted materials from the perspective of modern constitutive models. It also provides an evaluation of the capabilities of advanced numerical tools to reproduce the measured dam behaviour.

KEYWORDS: case history; compaction; dams; field instrumentation; numerical modelling

Le barrage de Lechago (à Teruel, en Espagne) est un structure en terre à zones et enrochements, placée sur des dépôts deltaïques continentaux tendres. Un noyau d'argile central relativement étroit est stabilisé par des épaulements à enrochements larges. Le barrage avait été bien instrumenté, et on dispose de relevés continus de développement de contraintes, pressions d'eau interstitielles et déplacements verticaux effectués au cours de la période de construction. On a suivi les conditions de compactage au moyen de tests de contrôle en laboratoire et « in situ », et examiné le noyau d'argile au moyen d'essais effectués sur des spécimens compactés d'argiles tertiaires. Des échantillons d'enrochement ont été excavés dans des affleurements de schistes quartzites du cambrien, extrêmement fracturés. On a mené un programme d'essais sur des graviers d'enrochement, avec humidité relative contrôlée, dans un oedomètre de grand diamètre et des cellules triaxiales. On a réalisé un modèle accouplé aux éléments finis pour analyser les tests effectués et le comportement du barrage au cours de la construction. On a effectué une comparaison des prédictions de modèle, basées essentiellement sur des essais en laboratoire, avec des mesures effectuées au cours de la construction. En outre, la réaction prévue du barrage soumis à un programme de retenue supposé est également fournie. Dans l'avenir, lorsque l'on procèdera à une retenue, il sera possible de comparer ces prédictions avec les performances effectives du barrage. La communication présente une description intégrée de la conception du barrage, de sa construction, et de son comportement initial, ainsi qu'une méthode d'interprétation des données disponibles (données relevées en laboratoire et « in situ ») sur des matières compactées, sous la perspective de modèles constitutifs évolués. Elle fournit également une évaluation des capacités des outils numériques perfectionnés pour la reproduction du comportement mesuré du barrage.

INTRODUCTION

Lechago dam, a 40 m high earth and rockfill structure (Fig. 1) was built in the period from April 2005 to January 2009. The first impoundment has been delayed to the first months of 2011. The flat upstream and downstream average slopes reveal the soft nature of the foundation soil in the central part of the dam. This situation was of special concern during design because it implied large total and differential settlements caused by the non-symmetrical cross-section of the valley and the stiffness of abutments, located in ancient shales and quarzitic rocks.

The design called for wide stabilising rockfill shells and a central clayey core. Fig. 2 is a photograph of the dam core, filter layer and the rockfill shoulder (shell) materials being compacted in situ. The maximum size of the gravel-like rockfill is about 20 cm but the mean particle diameter is close to 30–50 mm and therefore it may directly be tested in large-diameter laboratory cells, after removing the largest particles. Fig. 3 shows the grain size distributions of the in situ and tested rockfill material. The dam material had maximum sizes close to 9 cm and a somewhat increased content of fines, but otherwise the tested grading is quite similar to real conditions. Lechago rockfill material has been extensively tested during the past decade in the soil mechanics laboratory of Universitat Politècnica de Catalunya (UPC). The most salient feature of this experimental programme is the use of relative humidity (RH) control in the oedometer and triaxial tests performed. Some general results illustrating the effect of suction (or relative humidity) on the rock matrix and rockfill aggregate are collected in Figs 4–6. Brazilian tests on discs of rock equilibrated at different values of humidity were performed. The results (Fig. 4) show the variation of tensile strength with gravimetric water content or, alternatively, with total suction. Tensile strength increases the drier the specimen. Full wetting of an initially

Manuscript received 4 March 2010; revised manuscript accepted 21 December 2010. Published online ahead of print 22 March 2011. Discussion on this paper closes on 1 October 2011, for further details see p. ii.

* Department of Geotechnical Engineering and Geosciences. Universitat Politècnica de Catalunya, Barcelona, Spain
† Universidad Politécnica de Madrid, Madrid, Spain
‡ Confederación Hidrográfica del Ebro, Zaragoza, Spain

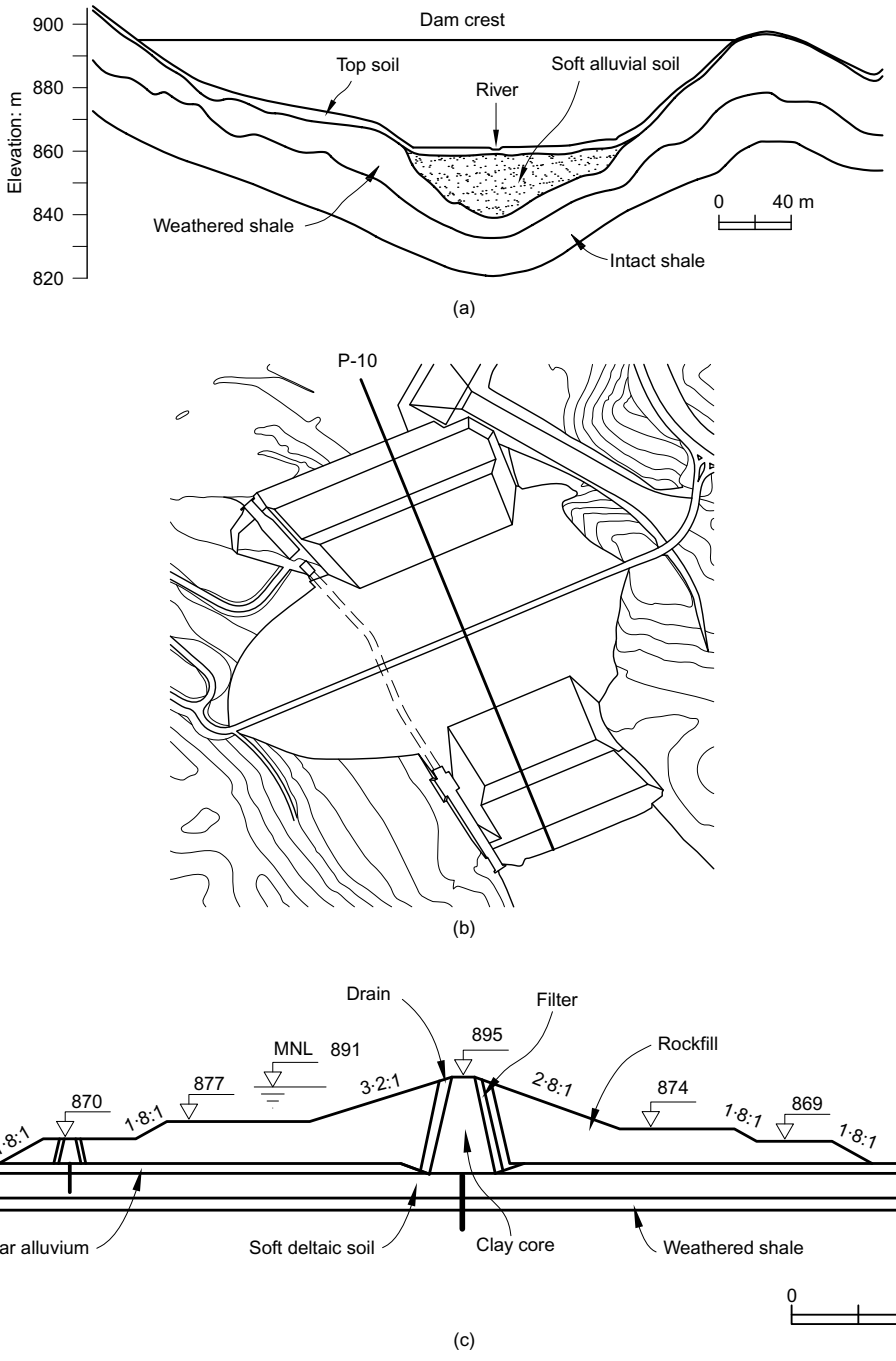

Fig. 1. (a) Valley cross-section; (b) plan view; (c) central cross-section P-10 of Lechago dam

dry rock reduces by half its tensile strength. The figure indicates the procedure to achieve a given humidity: equilibrating the rock specimen with salt solutions (indicated) or drying the specimens at the laboratory relative humidity (50%) (air) or submerging them in water.

Figure 5 provides the change in oedometric stiffness with applied total suction. It was found (Oldecop & Alonso, 2007) that the vertical stress–strain relationship could be approximated by a linear relationship

$$\varepsilon = \lambda \Delta\sigma \tag{1}$$

provided $\varepsilon < 8\%$. Rockfill specimens were compacted to an energy equivalent to standard Proctor energy. Compressibility also reduces substantially when the rockfill evolves from a very dry state (total suction, Ψ, equal to 255 MPa) to a saturated state.

The long-term deformation coefficient

$$\lambda^t = \frac{\mathrm{d}\varepsilon}{\mathrm{d}(\ln t)} \tag{2}$$

was also found to be linearly dependent on the compressibility coefficient λ.

However, the ratio λ^t/λ also depends markedly on current suction and it changes from 0·05 to 0·005 when suction changes from zero (full saturation) to $\Psi = 255$ MPa.

Figure 6 indicates the effect of RH on the strength envelope determined in a large-diameter triaxial cell on rockfill specimens compacted to standard Proctor energy (Chávez, 2004). The figure shows the expected curvature of the envelope. The effect of suction is in this case not so significant (RH = 36% is equivalent to $\Psi = 130$ MPa at 20°C from the psychrometric relationship).

A number of publications describe the relevance of RH in the behaviour of rockfill materials, the testing cells built and

Fig. 2. Clay core, filter and rockfill shoulder of Lechago dam during construction

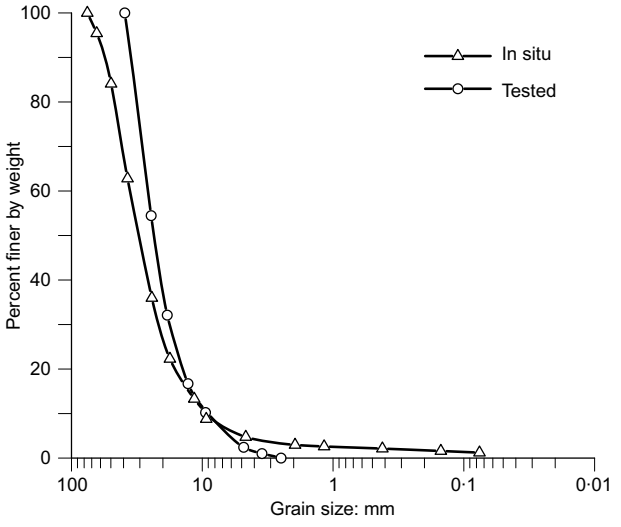

Fig. 3. Grain size distribution of Lechago rockfill material tested in the laboratory

the experimental results (Oldecop & Alonso, 2001; 2003; 2007; Chávez, 2004; Chávez & Alonso, 2003; Chávez *et al.*, 2009).

Piezometers (vibrating wire type), hydraulic settlement gauges and total stress cells were located in five cross-sections of the dam. The most detailed instrumentation corresponds to the central cross-section P-10, in the position of the maximum thickness of the soft alluvial deposits under the dam. Fig. 7 shows the instrument layout in section P-10. Surface topographic marks and levelling points were also located on the dam crest and downstream shoulders once the dam was completed.

Data recorded during dam construction will be later compared with the results of the model developed. Model parameters for the clay core and rockfill shoulders were derived from the analysis of tests performed on compacted clay from the core and the RH controlled triaxial tests reported in Chávez (2004). The foundation soil and, in particular, the soft alluvial clay and sand sediments were characterised at the design stage of the dam in the period 1998–1999.

The model has developed benefits from theoretical and applied contributions in the field of unsaturated soil mechanics performed by the authors and their colleagues in the past few years. The finite-element program Code_Bright,

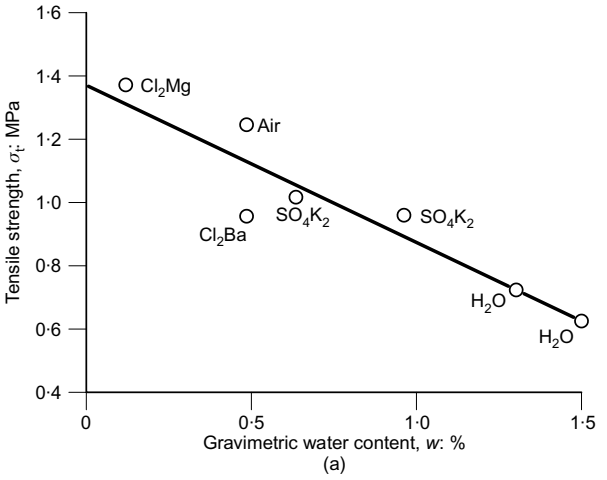

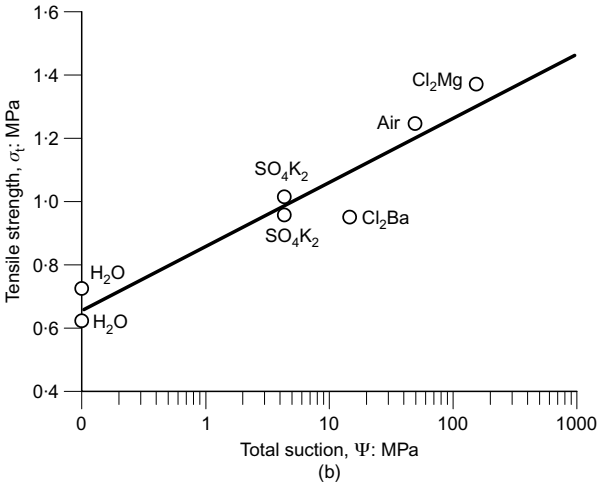

Fig. 4. Results from Brazilian tests on samples (84 mm diameter; 50 mm thick) in terms of (a) gravimetric water content; (b) total suction (Oldecop, 2000)

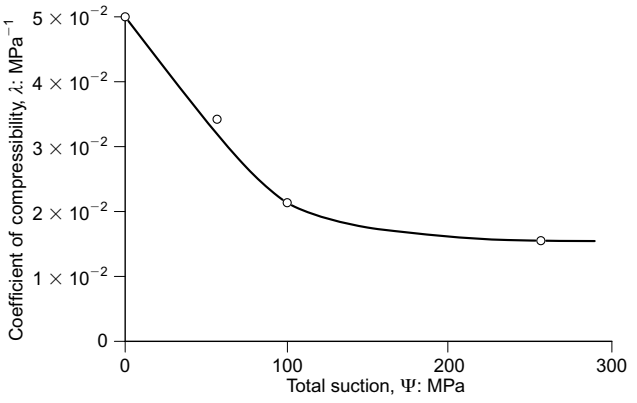

Fig. 5. Oedometric compressibility plotted against suction

whose basic formulation is described by Olivella *et al.* (1994; 1996) and DIT-UPC (2002) has been used in a variety of applications, including dam and embankment analysis (Alonso *et al.*, 2005) and nuclear waste applications (Olivella & Alonso, 2008; Gens *et al.*, 2009), among others. It handles in a unified manner saturated and unsaturated states and transitions between them.

The saturated foundation soils were characterised by a modified Cam-clay model. The central clay core was described by the so-called Barcelona basic model (BBM) for

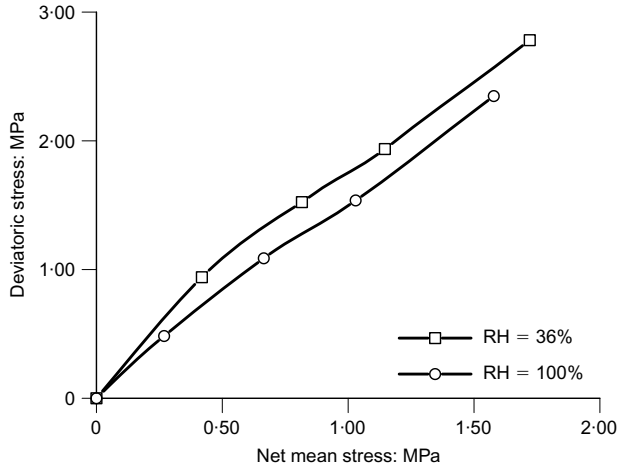

Fig. 6. Effect of RH on the strength envelope of compacted rock specimens in large-diameter triaxial cells

unsaturated soils (Alonso *et al.*, 1990). For rockfill shoulders and filters the isotropic elastoplastic model initially described by Oldecop & Alonso (2001) and later generalised to include deviatoric states in Alonso *et al.* (2005) was used.

The paper describes first a few relevant features of the dam design and construction, the foundation soils and field compaction data. Then, a back-analysis of large-diameter tests on compacted rockfill specimens and conventional tests on the compacted core clay is presented. Identified soil parameters are then used to simulate the dam construction. The model has been extended to simulate the first dam impoundment following a protocol that is often used in practice. The latter part of the paper provides a prediction of future dam performance, which may later be compared with actual dam performance.

DAM DESIGN AND CONSTRUCTION

The design of Lechago dam faced a number of challenging situations, namely the soft continental deltaic sediments filling the bottom of the valley, the marked non-symmetry of the valley, the sharp transition between highly deformable and rigid substrata and the fractured and pervious shale substratum in the entire area.

Earth dam construction on soft soil deposits is not common but several cases have been described in published papers (Daehn, 1985; Ramírez *et al.*, 1991; Rizzoli, 1991; Tellería and Gómez Laa, 1991; Torner and Novosad, 1991; Trkeshdooz *et al.*, 1991). Construction settlements in excess of 1 m have often been reported. In general, upstream and downstream slopes are controlled by global stability considerations and values in the range 4H–5H/1V are often found. This is also the case for Lechago dam.

Lechago has two definite cross-sections. On both sides of the central alluvial deposits a conventional zoned dam having 3·2H/1V and 2·8H/1V slopes (upstream and downstream) was designed. On the valley bottom this design was stabilised by wide rockfill berms to improve stability. In Lechago the project required a further improvement of the undrained strength of the soft alluvial deposits by means of a preloading operation of the downstream shoulders which would be carried out during construction. The actual construction involved a smaller preloading intensity than originally designed, supplemented by a water table lowering. Both operations were included in the model described below.

The actual construction sequence is plotted in Fig. 8 in terms of the evolution in time of the embankment height. In order to minimise differential settlements the design envisaged that the central section of the dam, directly founded on the soft alluvium, would be first built and then extended to occupy the valley slopes. However, in view of the fast consolidation of the alluvial soils, it was decided to build the dam in horizontal layers.

The three intermediate stops of construction activity shown in Fig. 8 were motivated by the difficulties in building the large spillway, excavated on the right abutment. The dissipation basin in the lower part encountered deep soft deposits and the construction involved a larger-than-expected excavation dewatering by means of deep wells and a piling foundation of the base slab. The downstream dam shell was affected and therefore the entire dam construction schedule was delayed. It was also decided to improve the foundation soils by reducing the water table under the downstream shell. The third and more extensive water lowering (third stop in Fig. 8) involved an average water table lowering of 2·5 m. In addition, surcharge preloading was resolved by a fill, 3 m high, emplaced on the downstream berms of the dam, at elevations of 869 and 874 m. Fig. 8 also indicates the measured piezometric level in the bedrock, below the dam downstream toe. Piezometric variations of about 3–4 m are a consequence of dewatering operations. The upstream

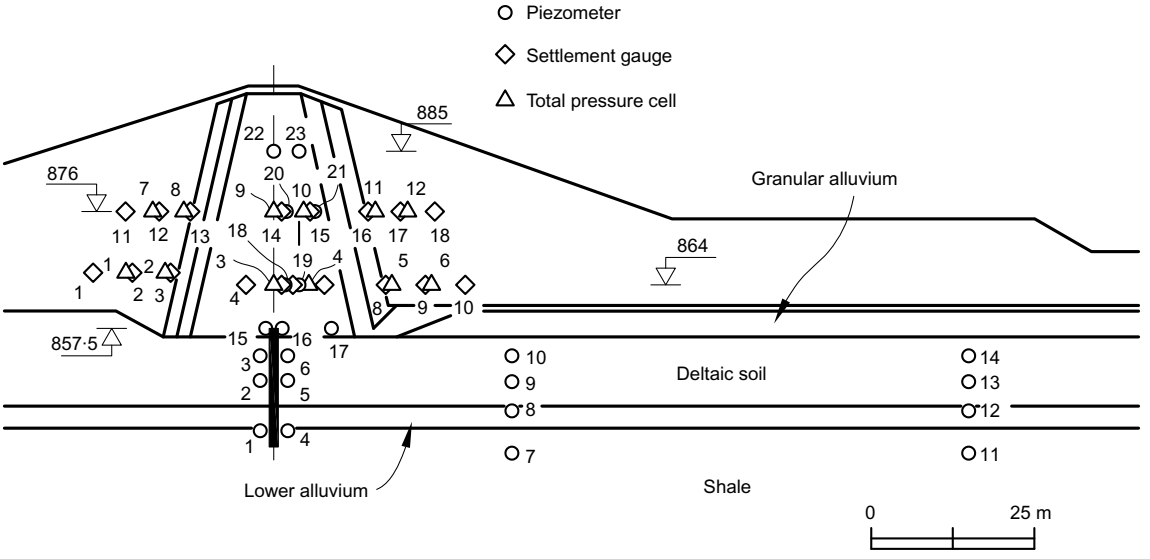

Fig. 7. Instrument layout in cross-section P-10

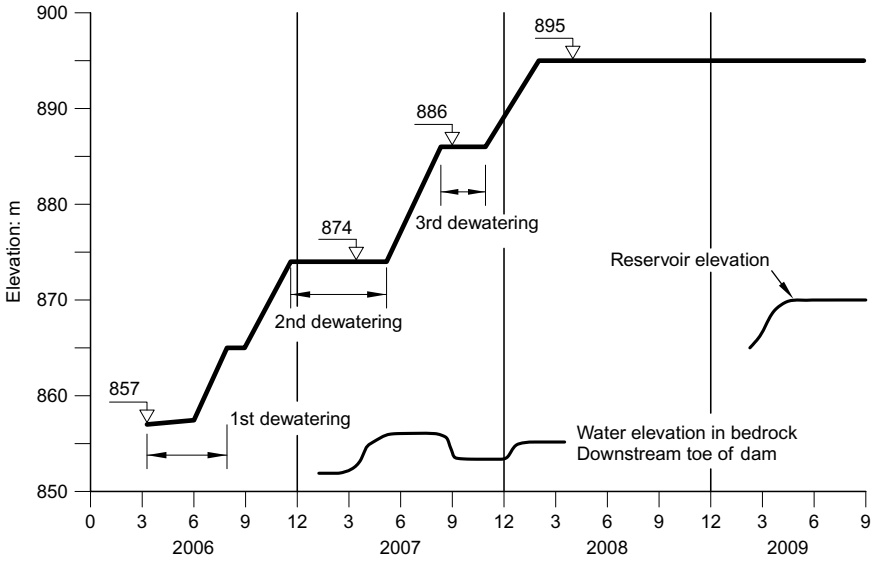

Fig. 8. Construction sequence

cut-off wall allowed a limited impoundment (beginning in March, 2009) as well, which is also shown in the same figure.

The dam reached its maximum elevation in March 2008, 24 months after the placement of the first compacted layer. The first control of dam surface settlements was performed in April 2009.

FOUNDATION SOILS AND CONSTRUCTION MATERIALS

The alluvium of the Pancrudo River was identified as a sequence of three horizontally layered strata: an upper layer of pervious sandy silt and gravels, 5 m thick, an intermediate soft clayey and silty stratum (deltaic deposits), 12 m thick, and a lower level of clayey sands and gravels 4 m thick directly over the shale substratum. In all levels thin sequences of impervious/pervious soils explain the fast consolidation of the entire alluvial stratum.

In the upper alluvium standard penetration test (SPT) values in the range 4–14 were measured. The central soft clayey stratum was often classified as low-plasticity clay (CL) or low-plasticity silt (ML), but clayey sands were also found. Void ratios range between 0·6 and 0·75. Liquid limit and plasticity index take values in the range 25–40% and 5–16% respectively. Critical stability conditions of the dam slopes were found under undrained conditions for this layer, whose virgin compression indices $C_c = 0{\cdot}15–0{\cdot}18$ were measured in standard oedometer tests. Horizontal consolidation coefficients in the range $c_h = 0{\cdot}6–6\ \text{cm}^2/\text{min}$ (0·01–0·1 cm^2/s) were obtained in CPTU dissipation tests. However, the frequent interlayering of sandy levels results in substantially higher representative consolidation coefficients. In fact, settlements of the base of the dam during construction increased in parallel with dam height. The lower thin alluvial sand was quite dense ($N > 30$).

The shale substratum was dissected by several faults which crossed the dam site. The upper decomposed and weathered shale level, 5–10 m thick, in contact with the alluvial or colluvial soils of the valley slopes, was moderately pervious ($k \approx 10^{-6}$ m/s, determined through Lugeon in situ tests).

A low-plasticity clay of Miocene age was selected for the dam impervious core. Dry densities not lower than 102% of the standard Proctor optimum value and water contents inside a ± 2% band around optimum were initially specified

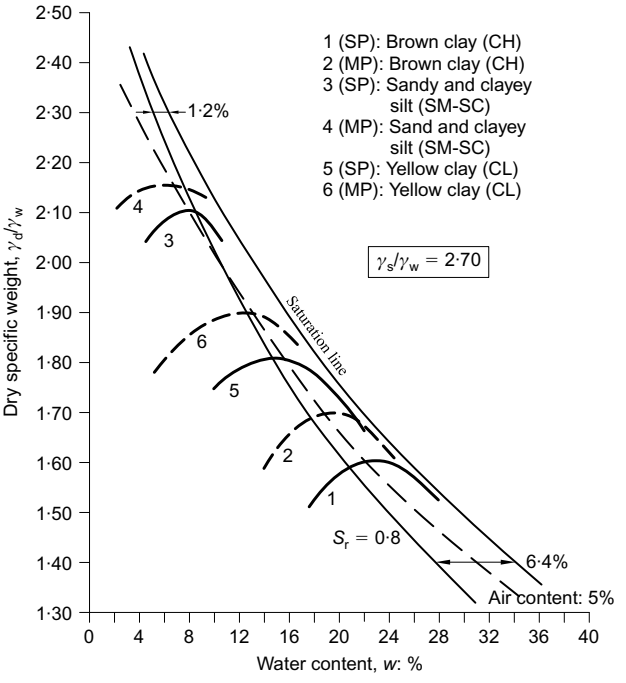

Fig. 9. Compaction tests on materials considered for the core of Lechago dam (SP: standard Proctor compaction; MP: modified Proctor compaction)

for construction. Fig. 9 provides a set of compaction curves, determined during the design stage, on Miocene clayey materials located in the vicinity of the dam. Standard Proctor (SP) and modified Proctor (MP) energies were used. The selected clay for the core was the yellow clay. It reached optimum dry unit weights of 18 kN/m^3 (SP) and 19 kN/m^3 (MP). In all cases optimum conditions correspond reasonably well to a 5% air content. The clay, after a period of exposure to natural weathering, was compacted in 25 cm thick layers by means of six runs of a sheep foot roller and a final run of a smooth roller (when the nuclear probe control measurements were required). In all cases the continuity of layers was ensured by a scarification of the current compacted surface prior to the placement of a new layer. The dry density limit was strictly enforced but water con-

tents were accepted in a wider range (−8% to +2% around optimum). The average compaction water content remained slightly below optimum.

Figure 10 provides the dry unit weight–water content in situ determinations during construction. Most of the dry unit weights remain in the range 18·7–19·7 kN/m^3 ($e_0^c \approx 0{\cdot}38$–$0{\cdot}45$). These values may be compared with the laboratory results in Fig. 9. Field compaction in the core reached densities in the vicinity of the MP optimum. The plot in Fig. 10 shows that the average degree of saturation during construction was around 0·9, a value close to optimum. A small proportion of the core volume seems to have degrees of saturation in the range 0·6–0·8, on the dry side of compaction.

Oedometer tests for specimens compacted to the range of γ_d values reached during construction provided the following compression indices: $C_c = 0{\cdot}07$–$0{\cdot}12$; $C_s = 0{\cdot}03$–$0{\cdot}05$. Measured coefficients of consolidation ranged between $c_v = 1{\cdot}5 \times 10^{-2}$ cm^2/s and $c_v = 3{\cdot}5 \times 10^{-2}$ cm^2/s. Derived permeability was in the range ($k \approx 2 \times 10^{-8}$ to 7×10^{-9} m/s). The measured secondary compression coefficient was a small proportion of C_c ($C_\alpha^c \approx 0{\cdot}013$–$0{\cdot}015 C_c$).

Collapse tests were also performed on several clay samples compacted to several dry specific weights and water contents. Samples were taken to vertical compression stresses of 100 and 400 kPa and were flooded at constant stress. The plot in Fig. 11 shows the measured collapse strains. The boundaries shown in the figure define three regions: very low collapse, medium to low collapse and medium to high collapse. The specimens tested cover a range of Miocene clayey materials having different grain size distributions and plasticity even if most of them are classified as CL or ML. Note that in all cases the collapse increases substantially when the vertical stress increases from 100 kPa to 400 kPa. The plot in Fig. 11 and the field density and water content data given in Fig. 10 indicate that the dam core has a low collapse potential (expected collapse strains smaller than 1% as a rough guide). This information was available at design stage and it was necessarily approximate because the objective at the time was to select the appropriate core material in the vicinity of the dam. More recently, tests were also performed on samples of the core material. The results will be analysed in the next section.

The quartzitic Cambrian shales used in the shells were highly fractured and the combined effect of quarry excavation, transport and placement in layers (40–50 cm thick) resulted in a gravel-like material (maximum sizes of the order of 10 cm). Therefore, compaction control tests could be performed in the laboratory in modified Proctor test moulds, removing the bigger fragments when necessary. The

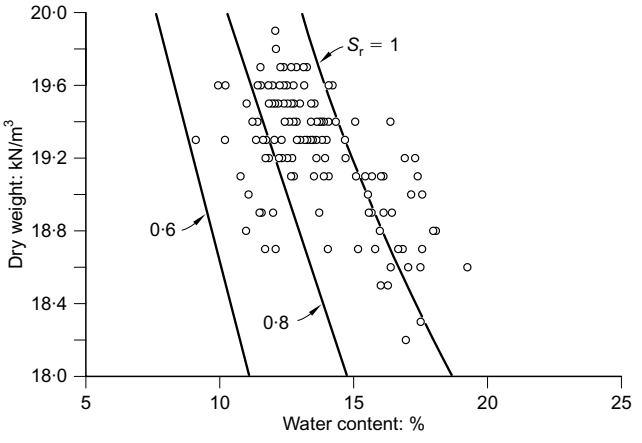

Fig. 10. Compaction data on core clay; in situ determinations

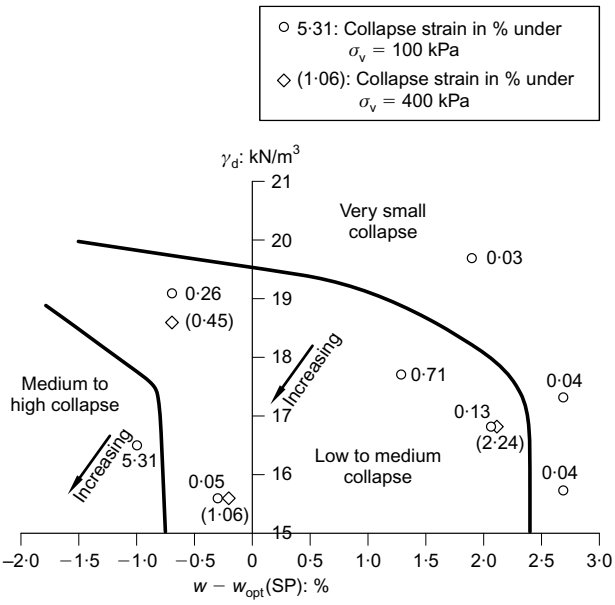

Fig. 11. Oedometer collapse of specimens compacted to the specified dry unit weight and water content (samples recovered in trenches at the design stage of the project)

modified Proctor optimum was taken as a reference for field control, which was carried out by means of nuclear probes that were calibrated by direct density and water content determinations at the beginning of construction works. The rockfill was compacted by a 19 ton vibratory roller (six runs for each layer).

The measured dry unit weights and water contents are collected in Fig. 12 in the conventional compaction plane. Water contents range between 6% and 7% for dry unit

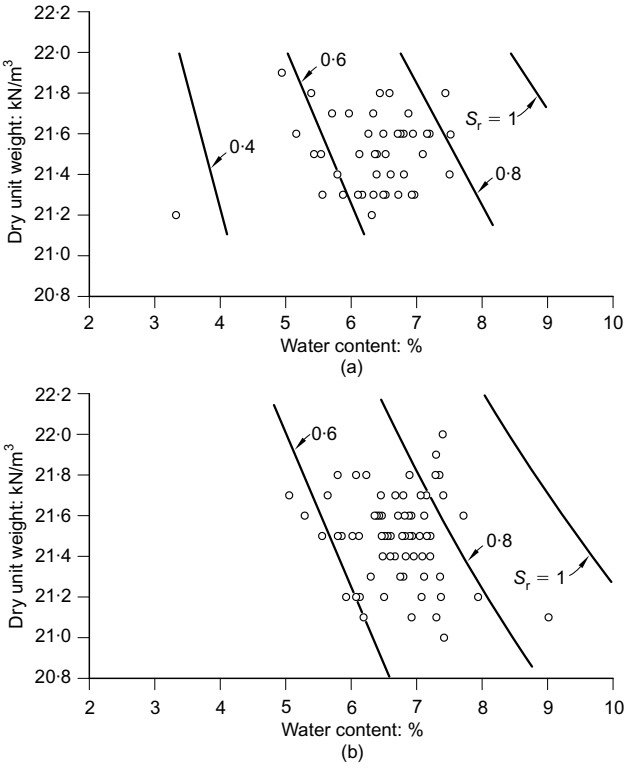

Fig. 12. Field compaction data for (a) upstream shell; (b) downstream shell

weights in the range 21–22 kN/m^3. The resulting degree of saturation varies between 0·6 and 0·8.

Oldecop & Alonso (2001) measured the water retention curve of Lechago shale gravel. They found that the porosity of the rock fragments amounts to 3·5–4%. Since the compacted rockfill has a global water content in the range 6–7%, if the rock fragments are saturated, some additional water partially fills the rockfill pores. This water is probably associated with the fines produced by the heavy compaction and/or by the insufficient drainage of the layer just compacted in situ at the time of the nuclear probe determinations.

The stress–strain behaviour of Lechago rockfill was tested in a RH-controlled large-diameter triaxial chamber, as described by Chávez (2004) and Chávez *et al.* (2009). Some isotropic and triaxial compression tests will be reproduced by the model developed in a next section.

TESTS ON COMPACTED MATERIALS AND THEIR INTERPRETATION

The available laboratory tests performed on the rockfill material and the clay core have been simulated as a boundary value problem with the help of the finite-element code Code_Bright with the purpose of determining material parameters. Table 1 provides a synthetic description of the models (BBM and rockfill model (RM)) used in the representation of the different materials.

Rockfill material

Triaxial samples, 250 mm in diameter and 500 mm high, were prepared by repeated compaction, applying an energy estimated at 600 J/m^3. The maximum size of particles was 40 mm. Samples were subjected to isotropic and triaxial loading at a specified relative humidity, which was controlled by imposing a vapour equilibrium technique (Oldecop & Alonso, 2001).

In order to simulate the tests performed, an axi-symmetric model of the actual triaxial specimens, described by quadrilateral linear elements, was developed. Stress, strain and flow conditions were applied at the specimen's boundaries as required.

Tests are treated as coupled flow and deformation boundary value problems. Both liquid flow and vapour flow were imposed to simulate the wetting of the samples following the test protocol in each case. The list of parameters required in the RM (Oldecop & Alonso, 2001) is indicated in Table 2.

The water retention curve introduced in the calculations, shown in Fig. 13, was based on the curve reported by Oldecop & Alonso (2001) for compacted specimens of the same rockfill. Because of the larger proportion of fines in situ (see Fig. 3) the air entry value was moderately increased, and more water was allowed to be retained at moderate suction values.

The water retention curve was simulated by means of a van Genuchten (1980) equation having a sub-horizontal shape for most of the accessible range of degrees of saturation. The smaller voids inside the rock particles retain water for low degrees of saturation, at high suction. The largest inter-particle voids provide the air entry value. Relative permeability was defined by means of the cubic law according to the following expression

$$k_{\mathrm{rel}} = k_{\mathrm{sat}}(S_{\mathrm{r}})^3 \tag{3}$$

where k_{sat} is the coefficient of permeability for saturated conditions and S_{r} is the degree of saturation.

The calibration of the remaining mechanical parameters indicated in Table 2 was obtained by a back-analysis of the laboratory tests. A comparison of model predictions and measured sample responses is shown in Figs 14–17.

Figure 14 shows the measured and simulated response of an isotropic test at constant suction performed in the triaxial apparatus. The saturated isotropic loading–unloading curve (Fig. 14(a)) shows the linear stress–strain relationship of the rockfill-type material and allows the calibration of the

Table 1. Basic relationships for constitutive models used in the analysis of Lechago dam*

	Barcelona basic model (BBM) (Alonso *et al.*, 1990)	Rockfill model (RM) (Compressibility part described by Oldecop & Alonso, 2001)
Isotropic elastoplastic volumetric deformation†	$\mathrm{d}\varepsilon_{\mathrm{v}} = \dfrac{\lambda(s)}{1+e}\dfrac{\mathrm{d}p}{p}$	For $p \leqslant p_{\mathrm{y}} \Rightarrow \mathrm{d}\varepsilon_{\mathrm{v}} = \mathrm{d}\varepsilon_{\mathrm{v}}^{i} = \lambda^{i}\mathrm{d}p$ For $p > p_{\mathrm{y}} \Rightarrow \mathrm{d}\varepsilon_{\mathrm{v}} = \mathrm{d}\varepsilon_{\mathrm{v}}^{i} + \mathrm{d}\varepsilon_{\mathrm{v}}^{d}$ $= [\lambda^{i} + \lambda^{d}(s)]\,\mathrm{d}p$
Volumetric compressibility index†	$\lambda(s) = \lambda(0)[(1-r)\exp(-\beta s) + r]$	$\lambda^{i} + \lambda^{d}(s)$ $\lambda^{d}(s) = \lambda_0^{d} - \alpha_{\mathrm{s}}\ln\left(\dfrac{s+p_{\mathrm{atm}}}{p_{\mathrm{atm}}}\right)$
Hardening law	$\mathrm{d}p_0^{*} = \dfrac{(1+e)p_0^{*}}{\lambda(0)-\kappa}\mathrm{d}\varepsilon_{\mathrm{v}}^{p}$	$\mathrm{d}p_0^{*} = \dfrac{\mathrm{d}\varepsilon_{\mathrm{v}}^{p}}{\lambda^{i}-\kappa}$
Loading–collapse curve (LC)	$p_0(s) = p^{c}\left(\dfrac{p_0^{*}}{p^{c}}\right)^{[\lambda(0)-\kappa]/[\lambda(s)-\kappa]}$	For $p_0^{*} \leqslant p_{\mathrm{y}} \Rightarrow p_0(s) = p_0^{*}$ For $p_0^{*} > p_{\mathrm{y}} \Rightarrow p_0(s) = p_y + \dfrac{(\lambda^{i}-\kappa)(p_0^{*}-p_{\mathrm{y}})}{(\lambda^{i}+\lambda^{d}(s)-\kappa)}$
Shear strength critical state parameter	$M(s) = M$	$M(s) = M_{\mathrm{dry}} - (M_{\mathrm{dry}} - M_{\mathrm{sat}})\left(\dfrac{M_{\mathrm{sat}}}{M_{\mathrm{dry}}}\right)^{s/(10\,p_{\mathrm{atm}})}$
Tensile strength parameter	$p_{\mathrm{s}}(s) = k_{\mathrm{s}}s$	
Yield surface (triaxial)	$F(p, q, s) = q^2 - M^2[p + p_{\mathrm{s}}(s)][p_0(s) - p] = 0$	
Plastic potential (triaxial)	$G(p, q, s) = q^2 - \alpha M^2[p + p_{\mathrm{s}}(s)][p_0(s) - p] = 0$	

*A common notation was used for equivalent parameters. Material constants are different for the soil and RMs.
†Suction, s, refers to matric suction in the case of BBM, and to total suction in the case of RM.

Table 2. Mechanical parameters for rockfill and drains

Definition of parameter	Symbol	Units	Base case for Lechago dam	
			Shell	Drain
(*a*) *Elastic behaviour*				
Elastic modulus	E	MPa	140	150
Poisson's ratio	ν	—	0·235	0·3
(*b*) *Plastic behaviour*				
Plastic virgin instantaneous compressibility	$(\lambda^i - \kappa)$	—	0·03	0·025
Virgin clastic compressibility for saturated conditions	λ_0^d	—	0·03	0·028
Parameter to describe the rate of change of clastic compressibility with total suction	α_s	—	0·0115	0·0115
Slope of critical state strength envelope for dry conditions	M_{dry}	—	1·8	1·7
Slope of critical state strength envelope for saturated conditions	M_{sat}	—	1·7	1·3
Parameter that controls the increase in cohesion with suction	k_s	—	0	0
Threshold yield mean stress for the onset of clastic phenomena	p_y	MPa	0	0·01
Parameter that defines the non-associativeness of plastic potential	α	—	0·25	0·3
(*c*) *Initial state for dam model*				
Initial suction	s_0	MPa	0·001	0·001
Initial mean yield stress (very dry conditions)	p_0^*	MPa	0·25	0·25

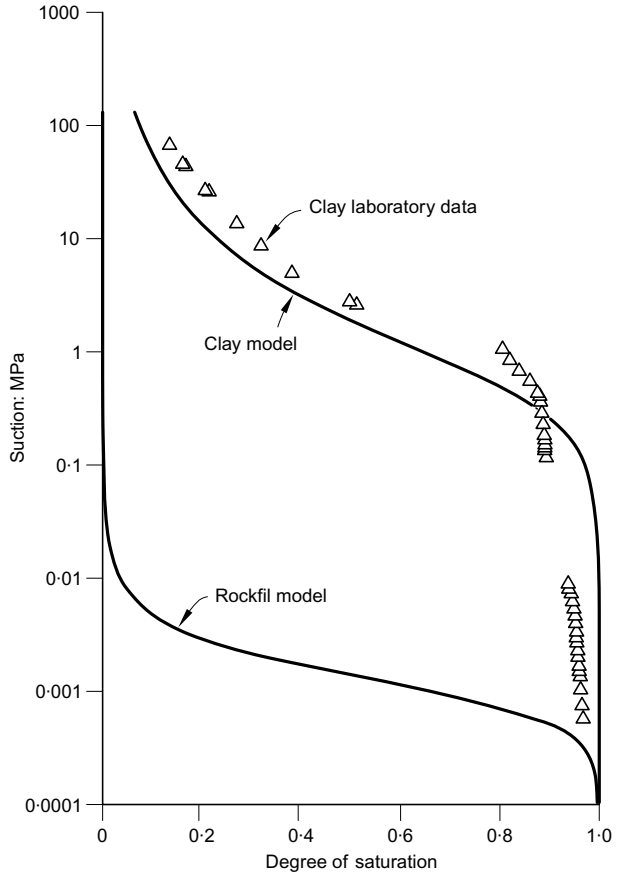

Fig. 13. Retention curves used in calculations for rockfill material and clay core

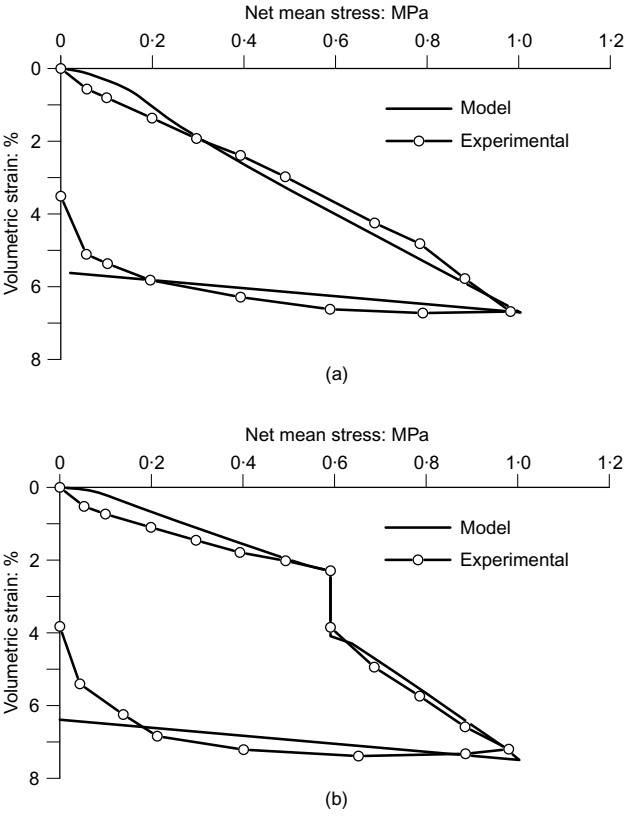

Fig. 14. Isotropic test: (a) saturated; (b) dry loading (RH = 36%) and saturation at a net mean stress of 0·6 MPa (experimental results by Chávez, 2004)

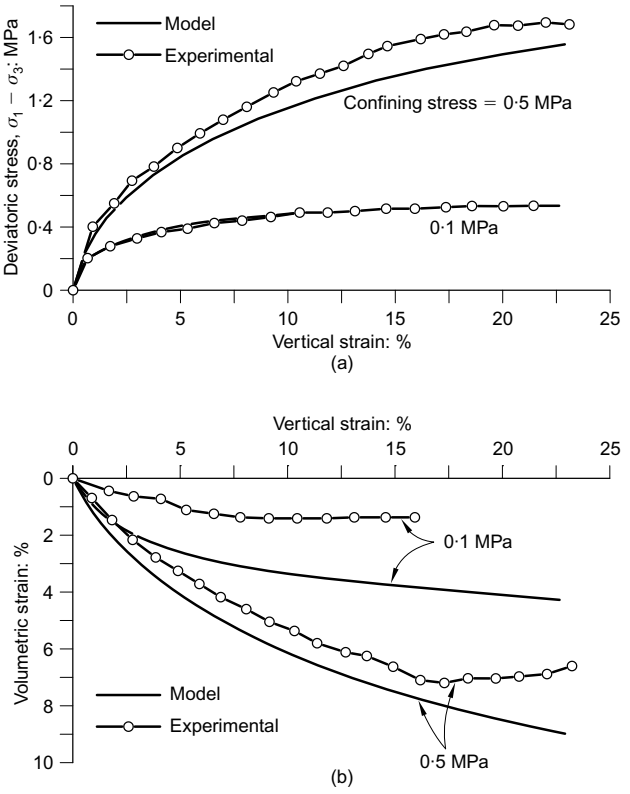

Fig. 15. Saturated triaxial test at two different confining stresses: (a) deviatoric stress–strain curves; (b) volumetric–axial strain curves (experimental results by Chávez, 2004)

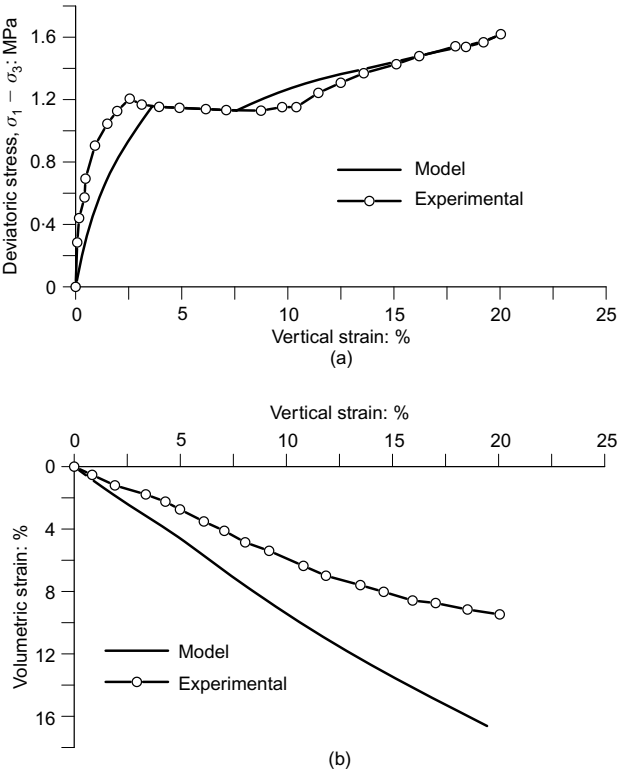

Fig. 17. Triaxial test at 36% RH and saturation at a confining stress of 0·5 MPa and constant deviatoric stress: (a) deviatoric stress–strain curves; (b) volumetric–axial strain curves (experimental results by Chávez, 2004)

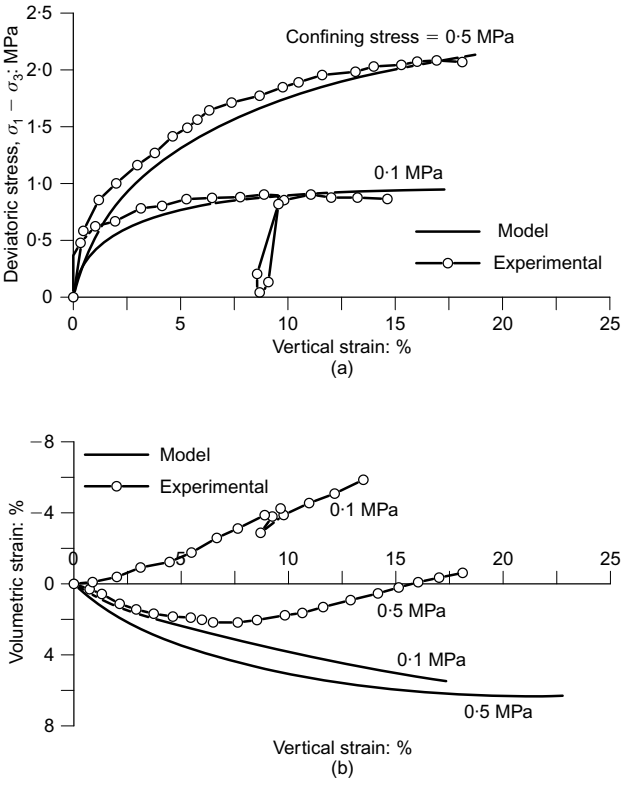

Fig. 16. Triaxial test at 36% RH and at two different confining stresses: (a) deviatoric stress–strain curves; (b) volumetric–axial strain curves (experimental results by Chávez, 2004)

compressibility parameters (λ_i and λ_0^d) and an estimation of the elastic modulus from the unloading curve.

In the second isotropic test (Fig. 14(b)), the sample was initially loaded at a maintained RH = 36%, which approximately corresponds to a value of total suction of 145 MPa according to the psychrometric relationship (Coussy, 1995). Suction was imposed during the first loading and the net mean stress was increased to 0·6 MPa. At this stress level the specimen was saturated. In the simulated test, saturation was reproduced by imposing a suction equal to zero at the top of the sample. The resulting water and vapour flow inside the sample was calculated by the model. Saturation of the sample resulted in a collapse of 2% volumetric strain, which was satisfactorily modelled (Fig. 14(b)). Hydraulic conditions were maintained during the remaining loading and unloading steps, which were performed under full drainage.

The first part of the compression curve at an imposed suction allows the estimation of the $\lambda(s)$ parameter, which describes the variation of compressibility parameter with suction and therefore the magnitude of collapse.

Figures 15 and 16 show the comparison between laboratory data and calculated values for triaxial tests performed at saturated condition and at 36% of RH respectively. The plots show the results for two confining stresses (0·1 and 0·5 MPa). The slope of the critical-state envelope (M) and its change with applied suction, was calibrated by means of the response of the material. A small increment of strength with suction was recorded. This is reflected in the values of M_{dry} and M_{sat} given in Table 2.

The non-associativeness of the plastic potential was estimated through the parameter $\alpha = 0{\cdot}25$. However, the dilatant behaviour was not well reproduced in all the simulated tests. The best approximation is obtained for the case of the

saturated triaxial test at a confining stress of 0·5 MPa (Fig. 15(b)). The behaviour exhibited by the drier specimen at a confining stress of 0·5 MPa (Fig. 16(b)), which initially contracted and then dilated without a marked softening in $p-q$ space cannot be properly reproduced by the implemented RM.

Finally, the triaxial test results given in Fig. 17 were simulated. The specimen was initially loaded in a dry condition (RH = 36%) under $\sigma_3 = 0{\cdot}5$ MPa and then saturated at constant deviatoric stress. The loading stage is resumed under saturated conditions. The parameters calibrated previously with the help of the tests described above were used. The model reproduces this singular test.

Clay core

Some tests were performed on the actual clay ($w_L = 38\%$, plasticity index (PI) = 18·5%) used in the core. Samples were compacted statically to densities of standard Proctor optimum. The optimum corresponds to a dry unit weight of 17·6 kN/m^3 and a water content of 17·8%.

Figure 13 shows the water retention curve obtained in the laboratory and the estimated curve introduced in the calculation using the van Genuchten model. The values of parameters (P_0 and λ) are given in Table 3.

Clay specimens compacted at standard Proctor optimum were tested in an oedometer test with suction control. The test results, plotted in Fig. 18, correspond to oedometric loading–unloading of a sample initially saturated at low level of stress (0·02 MPa). During saturation, the sample expanded. A second sample, compacted approximately at the same conditions, was first loaded at a constant suction equal to 1 MPa and then flooded at constant vertical stress (0·6 MPa) (Fig. 19). Model calculations are compared with experimental data in Figs 18 and 19. The clay behaviour was simulated using BBM (Alonso *et al.*, 1990).

Initial saturation at low stress level allowed an estimation to be made of the parameter κ_s, which controls the elastic volumetric strain for suction changes. Elastic and plastic

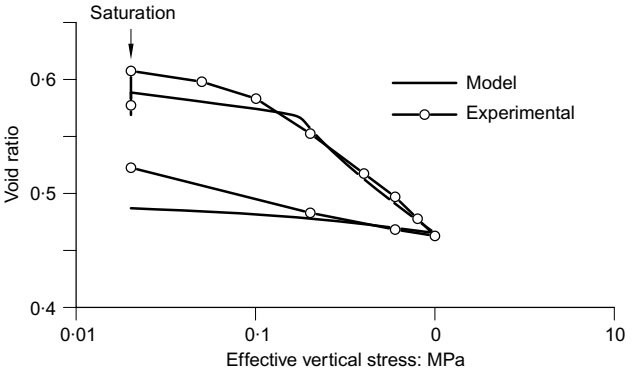

Fig. 18. Saturated oedometric test on a compacted clay sample initially saturated at constant vertical stress (0·02 MPa)

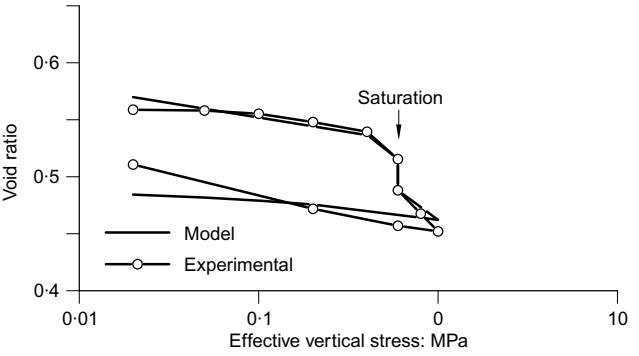

Fig. 19. Oedometric test on a compacted clay sample. Saturation at constant vertical stress (0·6 MPa)

compressibility parameters (κ and $\lambda(0)$) were estimated from the saturated test (Table 4). A comparison between saturated and unsaturated elastic compression curves indicates that the elastic stiffness increases with suction. This dependence has not been considered in the model. The model parameters which define the unsaturated compressibility and the shape of loading collapse (LC) yield surface (in the space net mean stress–suction) are estimated by means the unsaturated loading curve and the collapse intensity. Derived material parameters are collected in Table 4. The table also shows the set of parameters adopted for the natural foundation soil. They are based on field and laboratory data obtained at the design stage of the dam.

THE MODEL

A two-dimensional, plane strain, finite-element model of cross-section P-10 of Lechago dam was developed. The mesh used in calculations is made of linear quadrilateral four-node elements (Fig. 20(a)). Nodes have three degrees of freedom (water pressure, horizontal displacement and vertical displacement). The horizontal layers introduced to simulate construction and the dam materials are shown in Fig. 20(b).

Three materials define the dam: the clay core, the rockfill shells and the filters/drains. Four natural layers are distinguished in the foundation. Starting at the bottom, a stiff shale substratum ($E = 500$ MPa), 12 m thick, having a low permeability (3×10^{-9} m/s) is defined. Above this rock substratum, three soil layers are represented. Two permeable layers (4 and 4·9 m thick) of alluvium soil sandwich a less permeable soft soil (10 m thick). The upper permeable soil layer was excavated to build the clay core while the other two soil layers were cut by an impervious wall, connected with the clay core of the dam. The impervious wall was excavated by means of a slurry-trench technique and later filled with a cement–bentonite mixture, which was simulated by an elastic material (elastic modulus, $E = 100$ MPa; Poisson's ratio, $\nu = 0{\cdot}3$).

Table 3. Initial void ratio and intrinsic permeability adopted in calculations

Material	Initial void ratio, e_0	Intrinsic permeability, k: m^2	Retention curve, P_0: MPa	Retention curve, λ
Rockfill shell	0·43	1×10^{-12}	0·001	0·6
Clay core	0·67	1×10^{-15}	0·5	0·33
Drain	0·43	1×10^{-11}	0·01	0·33
Foundation soil: bed rock	0·43	3×10^{-16}	—	—
Foundation soil: alluvium soil	0·43	1×10^{-12}	—	—
Foundation soil: soft layer	0·54	1×10^{-14}	—	—
Cut-off wall	0·11	1×10^{-18}	—	—

Table 4. Parameters for the mechanical models used for the clay core and the foundation soils

Definition of parameter	Symbol	Units	Base case for Lechago dam			
			Clay core	Alluvium soil	Soft layer	Bed rock
(*a*) *Elastic behaviour*						
Elastic modulus	E	MPa	37	250	—	5000
Poisson's ratio	ν	—	0·3	0·3	0·3	0·3
(*b*) *Plastic behaviour*						
Elastic compressibility	κ	—	—	—	0·014	—
Virgin compressibility for saturated conditions	$\lambda(0) - \kappa$	—	0·046	0·01	0·055	—
Parameter that establishes the minimum value of the compressibility coefficient for high values of suction	r	—	0·7	—	—	—
Parameter that controls the rate of increase in stiffness with suction	β	MPa^{-1}	2	—	—	—
Elastic compressibility for changes in suction	κ_s	—	0·01	—	—	—
Reference stress	p^c	MPa	0·02	—	—	—
Slope of critical state strength line	M	—	0·85	1·2	0·85	—
Parameter that controls the increase in cohesion with suction	k_s	—	0·1	—	—	—
Parameter that defines the non-associativeness of plastic potential	α	—	0·3	0·3	0·3	—
(*c*) *Initial state for dam model*						
Initial suction	s_0	MPa	0·3	Saturated	Saturated	Saturated
Initial yield mean net stress	p_0^*	MPa	0·08	0·25	0·23	—

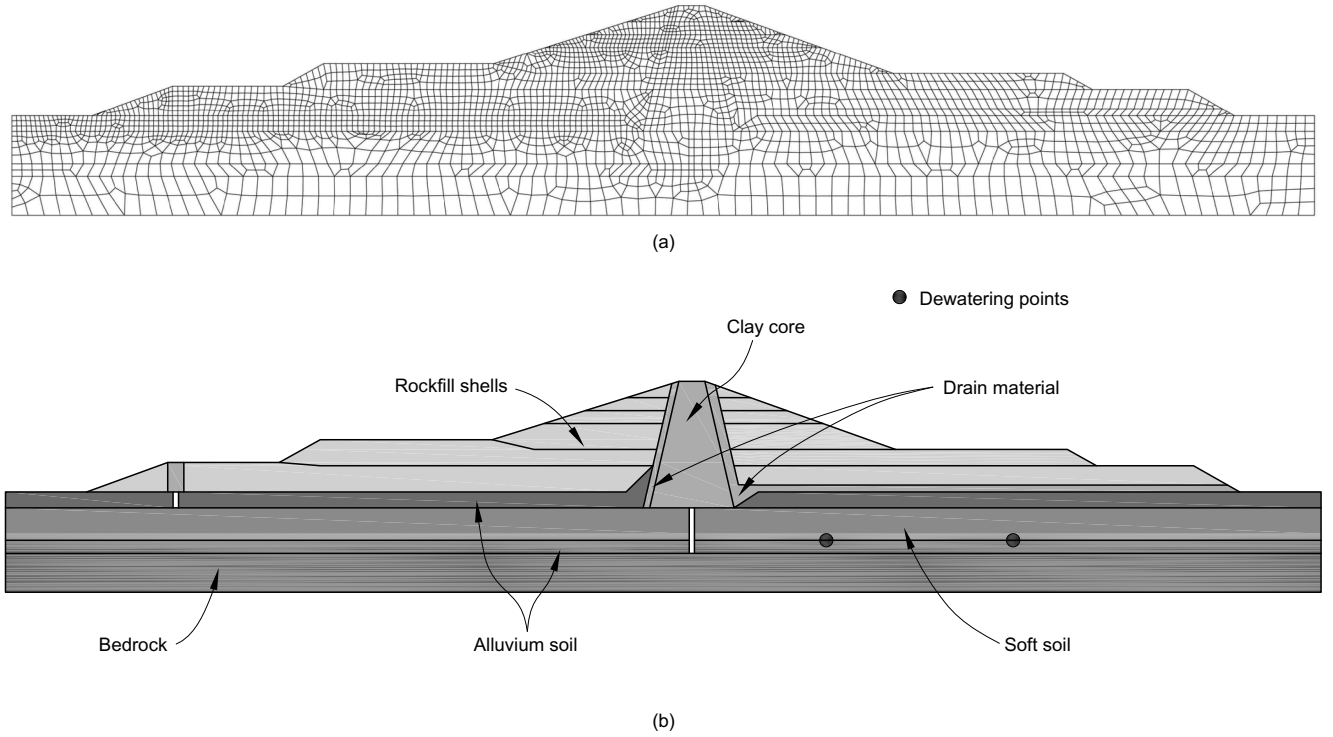

Fig. 20. Discretisation of cross-section P-10 of Lechago dam: (a) finite-element mesh; (b) materials and layers considered in construction simulation

Horizontal and vertical displacements were fixed at the lower plane of the model, which was considered impervious. Horizontal displacements were also fixed to zero and vertical displacements were free along the upstream and downstream vertical boundaries of the foundation.

The phreatic surface is located at the surface of the natural soil at the upstream side of the dam and 5 m below the surface at the downstream side. This jump in water table is created by the impervious wall and it was recorded by the piezometers installed. The water level is simulated by impos-

ing a hydrostatic pressure distribution on the lateral vertical boundaries of the foundation.

An initial geostatic total stress distribution on foundation soils was defined by a K_0 coefficient equal to 0·5. A preconsolidation mean effective stress (p_0^*) equal to 0·25 MPa has been defined for the pervious granular soil of the foundation and a slightly lower value, $p_0^* = 0{\cdot}23$ MPa, for the soft soil.

Construction was simulated by adding layers to the initial geometry of the foundation soils. The weight of each layer is applied in a ramped manner during the specified time period of its construction. The combination of steps and ramp loading gives a sufficiently realistic modelling. Each layer contains clay core elements, rockfill elements and drain elements, which were placed in between the core and shoulders. The dam was built in six steps (Table 5). The initial yield value of mean stress for dam materials should take into account the compaction stresses. For the clay core, the nominal value of the applied stress of the roller compactor, was used to define the initial mean stress, assuming $K_0 = 0{\cdot}5$. The RM requires the specification of the yield stress for very dry conditions. The selected value, $p_0^* = 0{\cdot}25$ MPa (Table 2), was approximated from the back-analysis of triaxial tests. The same parameter values were selected for filter materials.

Concerning initial suction the measured water content in situ (Fig. 10 for the clay core and Fig. 12 for the rockfill) and the water retention curves (Fig. 13) provide an approximate initial mean suction: 0·3 MPa for the clay core and 0·001 MPa for the rockfill.

In order to simulate the water level drawdown that was performed during construction to increase the preconsolidation stress of the soft deltaic deposits, two sink points (Fig. 20(b)) were included in this layer with the purpose of simulating the imposed drawdown by means of a water pressure reduction.

Before the construction of the two uppermost layers of the dam the preloading was simulated on the downstream side. Preloading was modelled through a vertical stress acting on the downstream slope surface. The preload was applied and removed, also using a ramp loading procedure to reproduce the construction and excavation process. During the 4 months of preloading time, dewatering in the lower permeable layer within the natural soil was simulated by means of 2·5 m water level decrease in the two sink points just below the preloading zone.

Granular drains are simulated by means of a RM and the material parameter values are given in Table 2. Compared with the rockfill properties, the sandy filters are assumed to be slightly stiffer and their frictional strength somewhat decreased. The downstream drain is simulated by means of a continuous layer which limits the clay core and continues below the rockfill shoulder to filter possible foundation water leaks and to avoid pressure development in the downstream shell.

BEHAVIOUR DURING CONSTRUCTION

Comparison between model performance and dam behaviour during construction will be based on stress measurements from total stress cells, vertical settlements determined by hydraulic gauges and pore pressure from piezometer readings. Hydraulic settlement gauges require a reference control position which was installed at the downstream edge of the horizontal berms at elevations 866 and 876 m. These points also experience settlements due to water table lowering and dam construction. The settlement gauges record the difference in elevation between a given gauge location and the reference position. The comparison made below refers to this difference in settlements. The reference control positions were levelled also by topographic procedures but the results were considered unreliable.

The total stress evolution recorded in some cells at some points has been compared with calculations. The comparison refers to several cells installed at the elevation 864–867 m. Fig. 21 shows the time records of measured stresses and their comparison with model predictions. The sudden reduction of the stress in the measurements at one of the gauges in the downstream rockfill (Fig. 21(c)) was attributed to an error in the instrument performance. Stress cells seem to provide in this case a fairly accurate indication of the dam construction history. In fact, the periods of rest between periods of construction activity are precisely detected. No significant delayed effects are shown by the readings. Vertical stresses within the clay core at the end of dam construction reach an average value of 0·4 MPa (two determinations). Recorded stresses in neighbouring points within the rockfill shells, close to the granular drains, show higher values, demonstrating the presence of arching effects due to the lower stiffness of the compacted clay core. Note that the dam geometry imposes a rapid change of height of compacted soil away from the core and arching effects develop. The model captures reasonably well the entire set of measurements. Of course, the large recorded stress variations within points close to each other (see, for instance, the records for the two stress cells within the clay core) cannot be reproduced by the model. In other respects the model is remarkably accurate. The model does not predict any significant delayed behaviour of stress development in the rockfill shells, as recorded. However, arching effects induced by the consolidation of the lower part of the clay core result in a calculated decrease of the vertical stresses, a phenomenon not observed in the field. Pore pressures in the core will be discussed below.

Table 5. Construction stages

		Model time	Dates	Modelling interval
Equilibrium of initial conditions		Time 0–100 days		1
Construction until elevation 874 m (see Fig. 1)		Time 100–280 days	1 July 2006–30 December 2006	2 3
Stop construction: Construction until elevation 886 m (see Fig. 1)		Time 280–460 days Time 460–520 days	1 January 2007–30 June 2007 1 July 2007–30 September 2007	4 5 6
Phreatic level red. and pre-loading	Pre-loading ramp Pre-loading Unloading	Time 520–560 days Time 560–620 days Time 620–640 days	1 September 2007–30 December 2007	7 8 9
Final construction (until elevation 895 m) (see Fig. 1)		Time 640–680 days Time 680–700 days	1 January 2008–30 February 2008	10 11

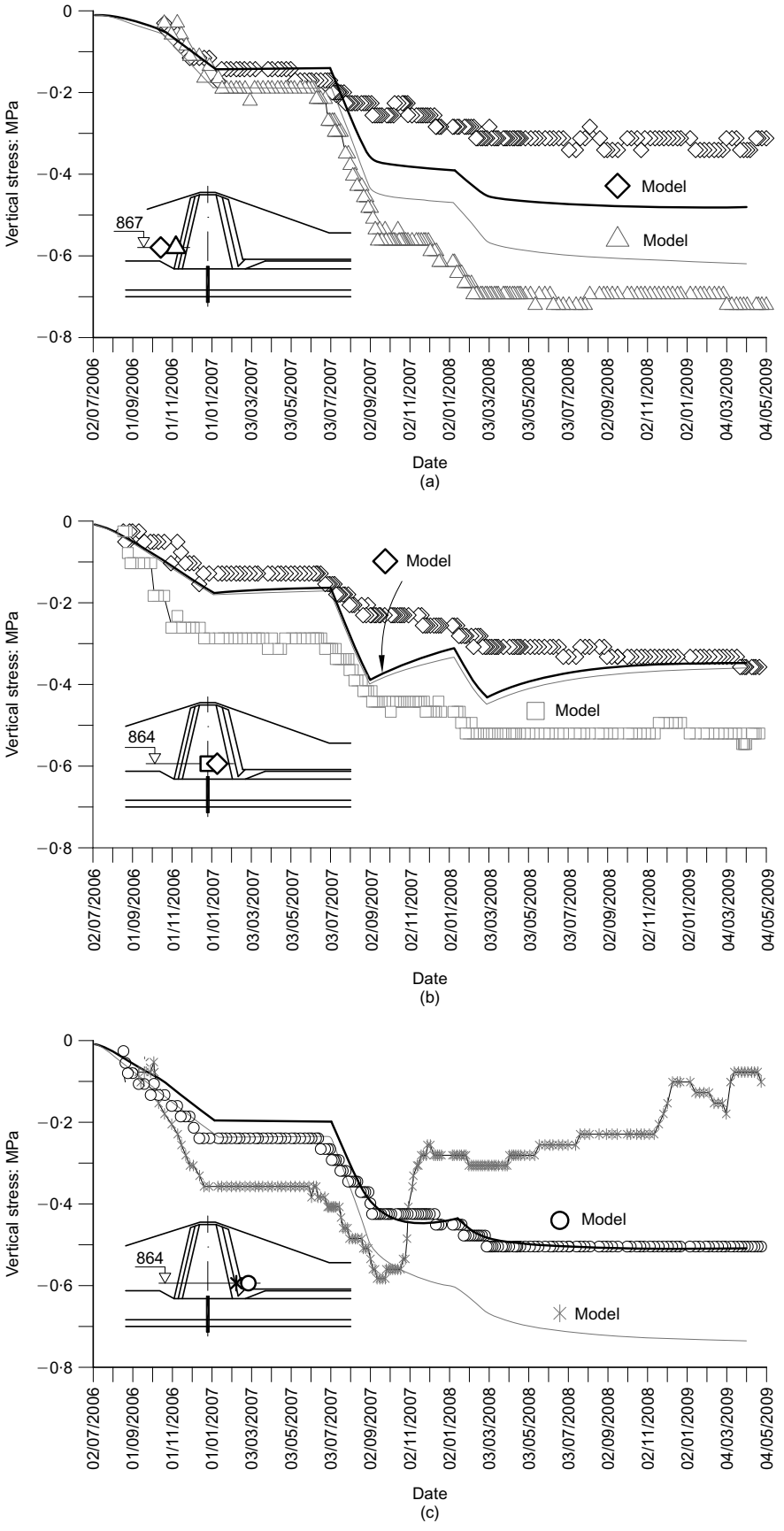

Fig. 21. Comparison of measured and calculated vertical stresses at elevation 867–864 m: (a) upstream rockfill near core; (b) clay core; (c) downstream rockfill near core

Figure 22 shows the calculated distribution of vertical stresses in the dam at the end of construction. Arching effects reduce the reference geostatic distribution of stresses in the core.

Calculated vertical displacements at elevation 876 m are compared with measurements in Fig. 23. In the upstream zone, near the core, measured displacements are somewhat overestimated by the calculated absolute displacements in the corresponding points. The reference for measurements was a fixed point in the slope of the valley. In contrast, in the case of the clay core and the downstream shoulder, the calculated values had to be corrected by substracting the settlement in the location where the reference measurement system was installed, as described above. Obviously this is not the best reference point but it had practical advantages. This situation can lead to measured values which apparently indicate an uplift of the soil, although all points experience settlements at all times. This trend is observed in the measured settlement records and it is more exaggerated in the calculations made. However, the magnitude of the measured values is in general well captured. Settlement records also react to the step-wise history of loading, but in a more progressive manner than the total stresses owing to consolidation effects in the foundation and the compacted structure.

Pore-water pressures are calculated and compared with measurements in Fig. 24. Piezometers could only measure small pressure deficiencies below the atmospheric value. In practice only positive values are measured. Consider first the piezometers located in the saturated foundation soil in vertical borings (Figs 24(a) and 24(c)). The measured time records reflect, in general, a hydrostatic distribution of pore pressures, controlled by the position of the water table. The dewatering period, especially the third one (final months of 2007), is reflected in all measurements. The model also reacts in a similar way.

The piezometer close to the base of the clay core, upstream of the cross-sectional axis (elevation 854·5 m) is interesting because it shows a steady increment of pore pressure due to the pore pressures accumulating slowly in the compacted core. The model calculations follow a sharper rate of pressure accumulation: pressure starts in a negative value (suction) but evolves rapidly to a positive pressure, which increases slowly and also follows the dewatering episodes.

The response of the clay core is plotted in Fig. 24(b). Piezometers located in upper levels (elevations 875·4 and 885 m) cannot record the prevailing suction. The model calculates suction values not shown in the figure because of the pressure scale of the graph. The piezometer located in the vicinity of the foundation (elevation 857 m) soon starts to record positive pore-water pressures. Model calculations start at the compaction suction and they show a progressive decrease in suction and, at some time during construction, the development of positive pore pressures. The model reacts to the rapid increase in total stresses by increasing the pore pressure (or by reducing suction). One period of rapid accumulation of stress was June–September 2007. It can be followed in the calculated response of the model but also on the reaction of the piezometers at lower elevation (857 m). The fast reductions in suction and the transient period towards a new equilibrium predicted by the model do not compare well with measurements. Interestingly, the piezometer at a higher elevation (864 m) begins to record positive pore-water pressures some time after the completion of the dam, in November 2008. This is not well captured by the model, which predicts an earlier development of positive pore pressures. The recorded increase of pore pressures at the end of the time period represented in Fig. 24 reflects the water level elevation upstream (6 m), which took place in March–April 2009.

Figure 25 shows the calculated distribution of pore-water pressures in the core at the end of construction. The model predicts a limited development of positive pore-water pressures in the lower third of the clay core. This result may be compared with the average value of recorded pore pressures in four cross-sections of the dam. The measured pore pressures in all four sections, in February 2008, once the dam was completed, have been plotted together by superimposing, averaging and smoothing the measurements (Fig. 25). The scatter of results in a given section and the limited number of piezometers installed makes this approach a reasonable one to derive an integrated and global picture of the core hydraulic behaviour. Piezometers were located in the downstream half section of the core and therefore no information on the upstream half is available. The calculated response is plotted in Fig. 25 for two dates: February 2008 and April 2009. The model predicts higher pore pressures in the lower part of the core, although it correctly predicts that the upper two-thirds of the dam core remain unsaturated. Once the dam was completed, calculated excess pore pressures dissipate at a relatively fast rate. This dissipation and the associated core settlement was the reason for the transient stress reduction shown in Fig. 21(b). Measured pore pressures were lower and their recorded dissipation was very slow. This discrepancy may be explained by a lower-than-assumed compacted water content in shells and core and also by errors in the assumed water retention and permeability parameters of both materials. However, no attempt to modify them in order to fit the actual measurements was made.

PREDICTION OF DAM BEHAVIOUR DURING IMPOUNDMENT

The protocol for dam impoundment has not yet been defined for Lechago dam. The assumption made here is that impoundment takes place at a maintained rate of 0·1 m/day until the maximum elevation (892 m). Figs 26–28 show the calculated response of the dam in terms of vertical stresses, vertical displacements and pore-water pressures. The plots

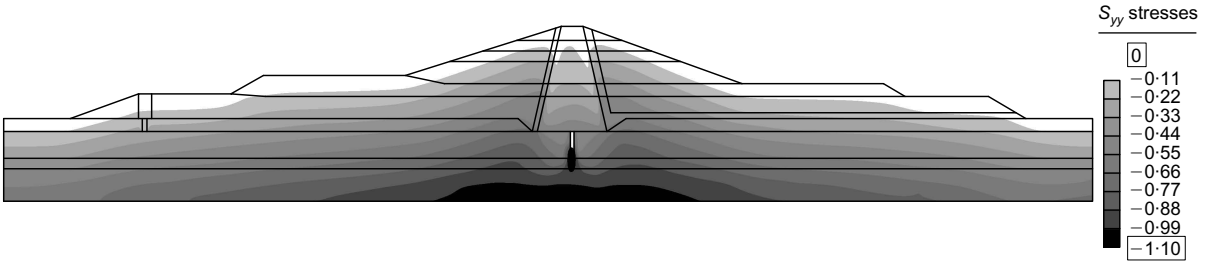

Fig. 22. Calculated contours of vertical stress at the end of dam construction

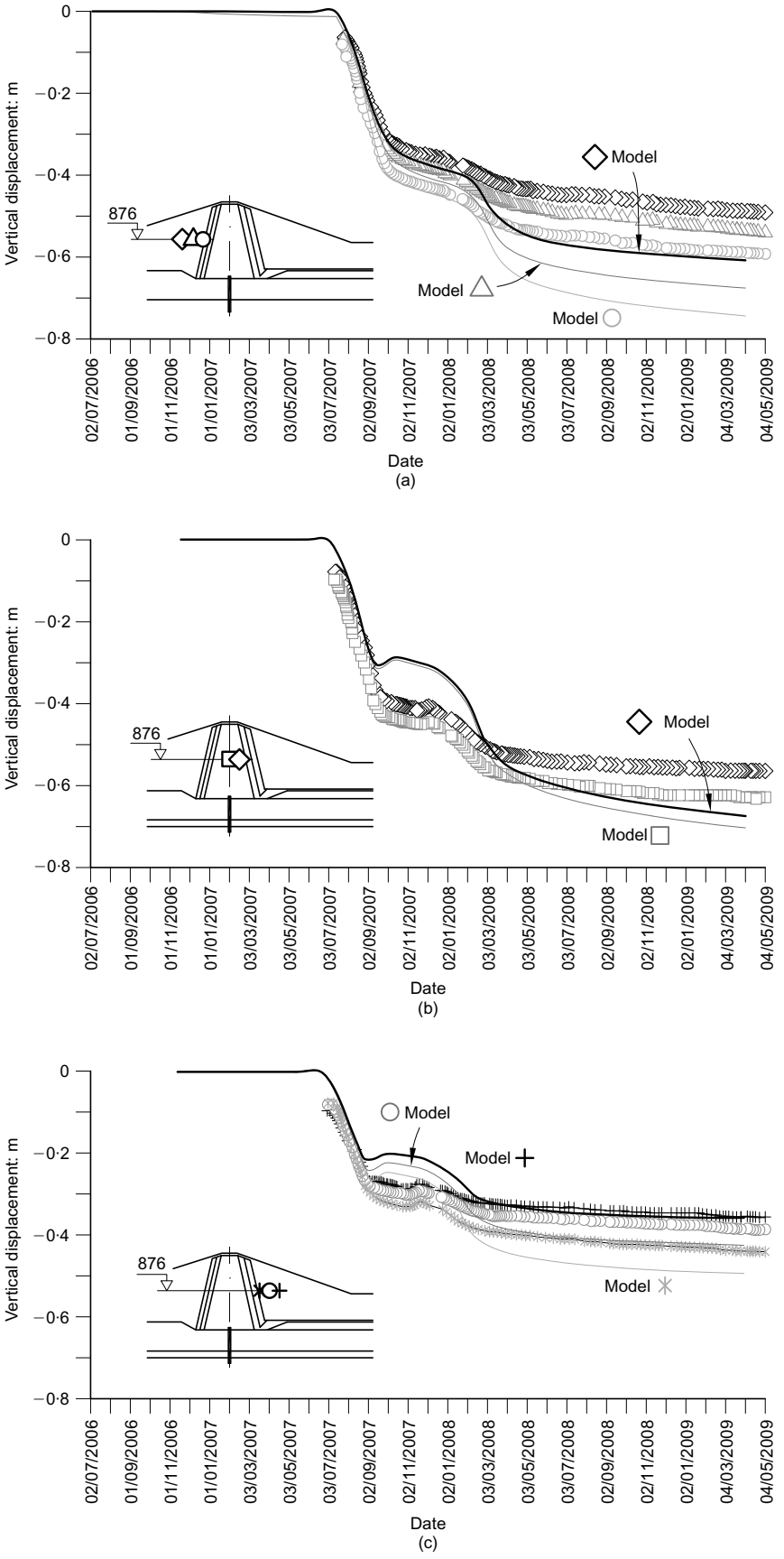

Fig. 23. Comparison of measured and calculated differences of vertical displacements between the measurement gauge and the reference location, elevation 876 m: (a) upstream rockfill near core; (b) clay core; (c) downstream rockfill near core

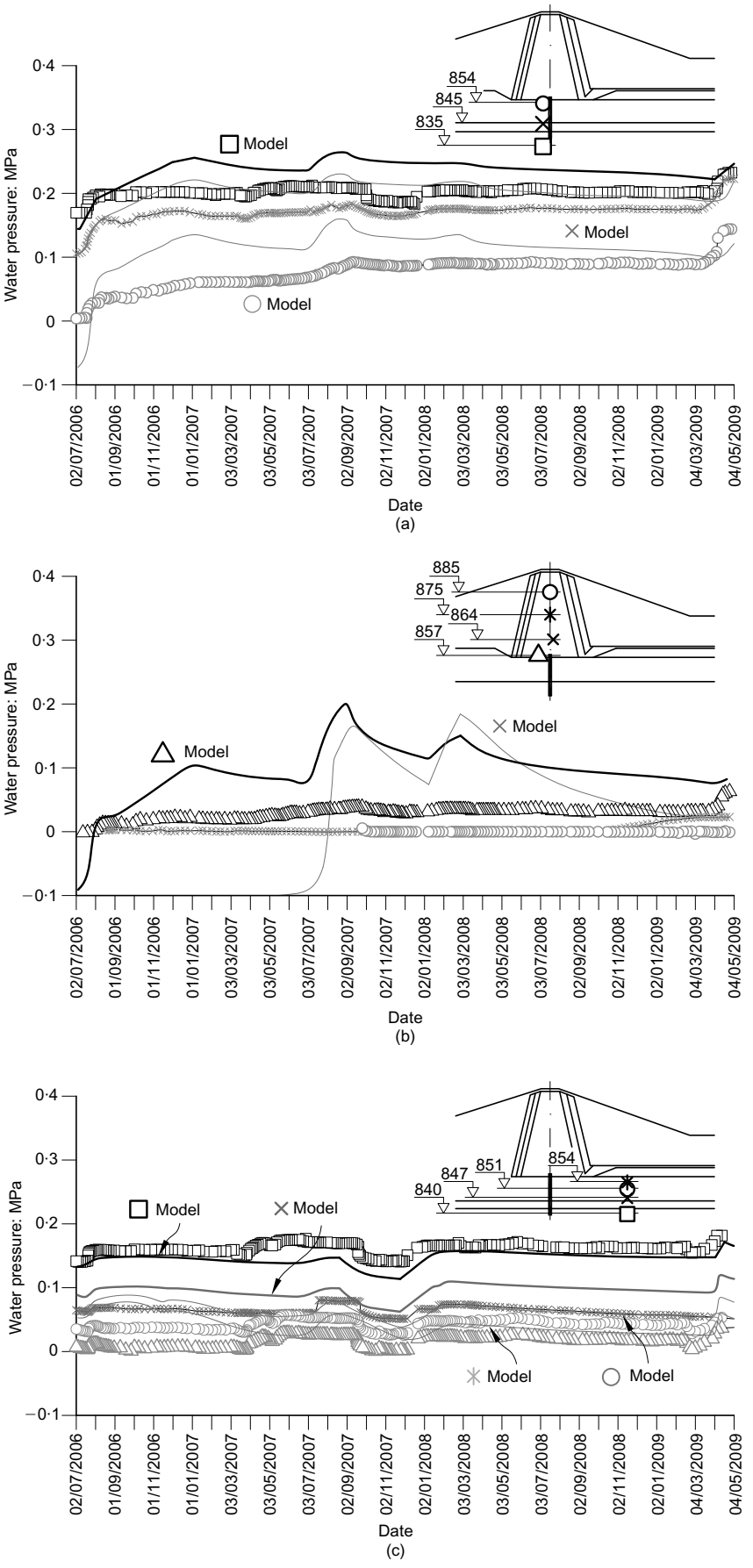

Fig. 24. Comparison of measured and calculated pore-water pressures in the locations indicated: (a) foundation soils, under the core; (b) clay core; (c) foundation soils, downstream

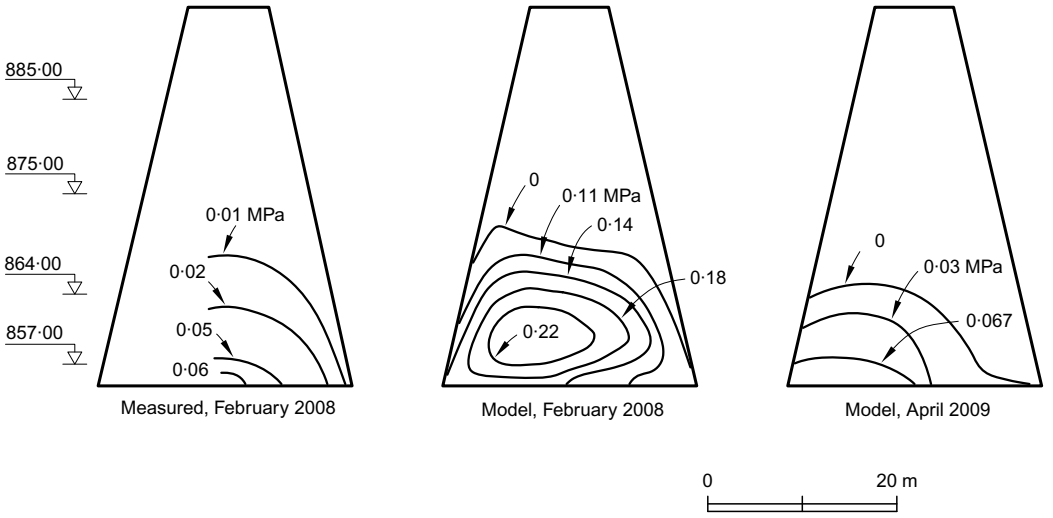

Fig. 25. Average measured pore pressures in cross-sections P-8, P-10 and P-12 in February 2008 and computed results in February 2008 and April 2009

refer to the position of instruments in the central cross-section of the dam, given in Figs 21, 23 and 24. The time origin in Figs 26–28 is the final calculation time for the construction phase. This origin may change when the actual impoundment starts.

Figure 26(a) shows a moderate increase of stresses at elevation 867 m, upstream of the core, due to the increase in total unit weight of the shell during its saturation. Inside the core (close to saturated conditions) and downstream the expected change in stresses is very small. Collapse-induced settlements calculated at elevation 876, are very small and a slight heave is predicted due to reduction of effective stress during impoundment (Fig. 27(a)). Downstream the expected settlement is even smaller. The maximum response concerns expected water pressures. The points within the foundation follow essentially the hydrostatic increase in pressure (Fig. 28(a)). The core is progressively saturated and pore pressures change from negative (suction) to positive values in the manner indicated in Fig. 28.

CONCLUSIONS

Lechago dam integrates widely different materials: a soft saturated clay foundation, wide rockfill shells to ensure stability and a core of compacted, medium-plasticity Miocene clay. Material properties could be derived from different sources. The dam provision process followed standard practice, which provided initial information on the properties of the foundation soils, the clay core and the rockfill.

Rockfill behaviour, however, was investigated in more detail and large-diameter tests on compacted specimens of the quartzitic shale used in the shells became available. These tests were performed under RH control, following recent developments which highlight the relevance of this variable to control the constitutive behaviour of coarse granular aggregates. The highly fractured quartzitic shale led, after quarrying, to a coarse gravel-like granular material whose grain size distribution can be reasonably well reduced to be tested in a 25 cm diameter triaxial cell.

Triaxial tests on rockfill have been simulated by discretising the specimens and following the actual sequence of RH changes and load increments. The RM used reproduces satisfactorily the isotropic stress–volumetric strain as well as the deviatoric stress–strain records. Difficulties are found in capturing the measured dilatancy.

Conventional wetting under load oedometer tests was simulated in a similar way to derive material parameters for the clay core.

The central cross-section of the dam was discretised and the actual construction sequence was applied. Specific features of Lechago construction are the preloading of the downstream shell to improve the undrained strength of the soft foundation deposits and the dewatering of the foundation soils for the same purposes. These operations resulted in a staged construction of the dam, which lasted 2 years.

The comparison between dam performance and model calculation involved three types of measurements in time: vertical total stress in core and rockfill, settlements of the dam at different levels and (positive) pore-water pressures in the clay core. These measurements are available at different elevations and at several vertical profiles in the natural foundation soils.

Measured vertical stresses were remarkably consistent despite the difficulties often encountered with these instruments. They indicated some arching phenomena in the softer core, which was captured by the model. Stress developments also closely matched calculations in most cases.

Settlement includes the response of the soft foundation and the compacted structure. Despite the difficulties in matching actual field conditions with the laboratory experiments available, the model performance is reasonably good. Lechago experienced large total settlements close to 1 m in the central section.

Pore-water pressures in the core cannot be determined unless they reach positive values. This prevents the proper evaluation of model performance in the unsaturated regions. However, the development in time of positive pore pressures (starting at a condition of partial saturation) is an indirect and useful check of the calculations. It has been shown that the lower third of the core develops positive pore pressures in the range 0·01–0·06 MPa (the latter in the base of the dam core). The model also predicts positive pore-water pressure developments in the lower part of the dam. This is a check and a further validation of the model and the set of parameters selected.

However, there are difficulties in practice which cannot be overlooked. At the design stage properties of compacted materials are established on the basis of a few laboratory tests performed in a variety of specimens with the purpose of selecting the most appropriate soil type. Later, field

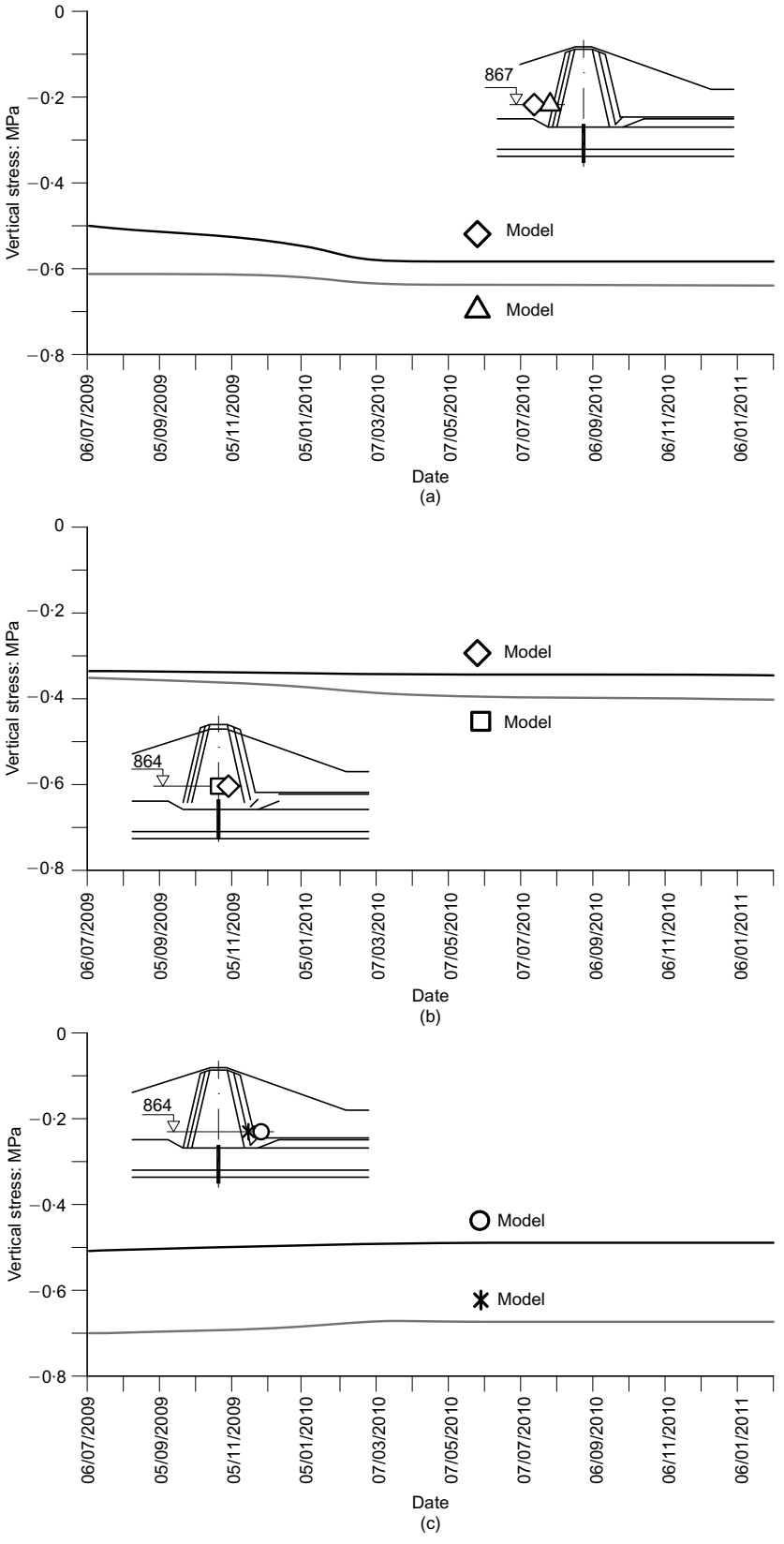

Fig. 26. Calculated vertical stresses at elevation 867–864 m during dam impoundment: (a) upstream rockfill near core; (b) clay core; (c) downstream rockfill near core

compaction techniques and specifications may experience significant changes if compared with the project specifications. Lechago is not an exception.

Attained densities, reference compaction energies and water content limits were modelled to a certain extent. The natural variability of quarries adds further uncertainties. Therefore, the reasonable response of the model and its satisfactory comparison with some measurements may include some fortuitous coincidences.

The model was used to explore the future behaviour of

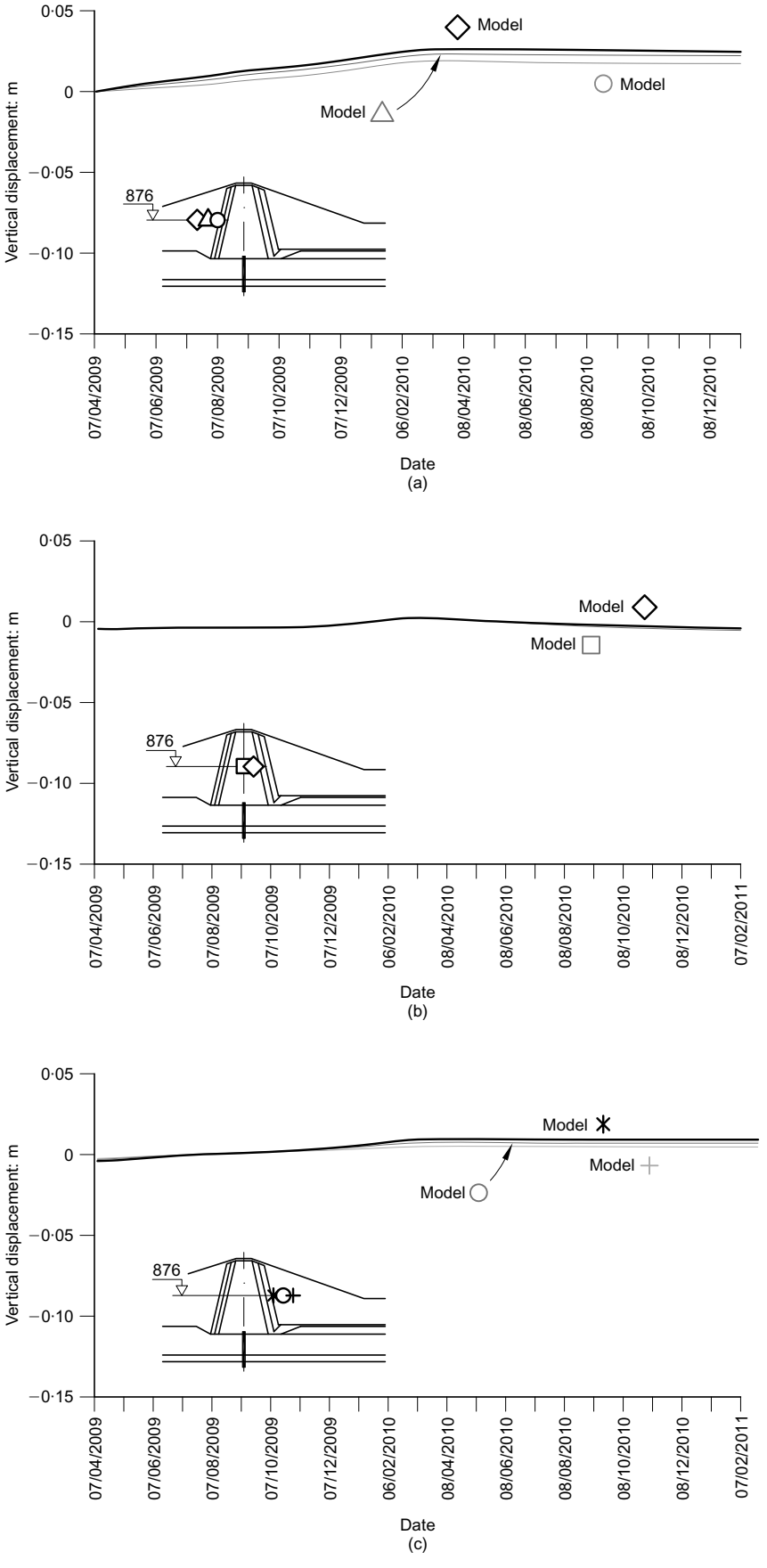

Fig. 27. Calculated differences of vertical displacements between the measurement gauge and the reference location during dam impoundment, elevation 876 m: (a) upstream rockfill near core; (b) clay core; (c) downstream rockfill near core

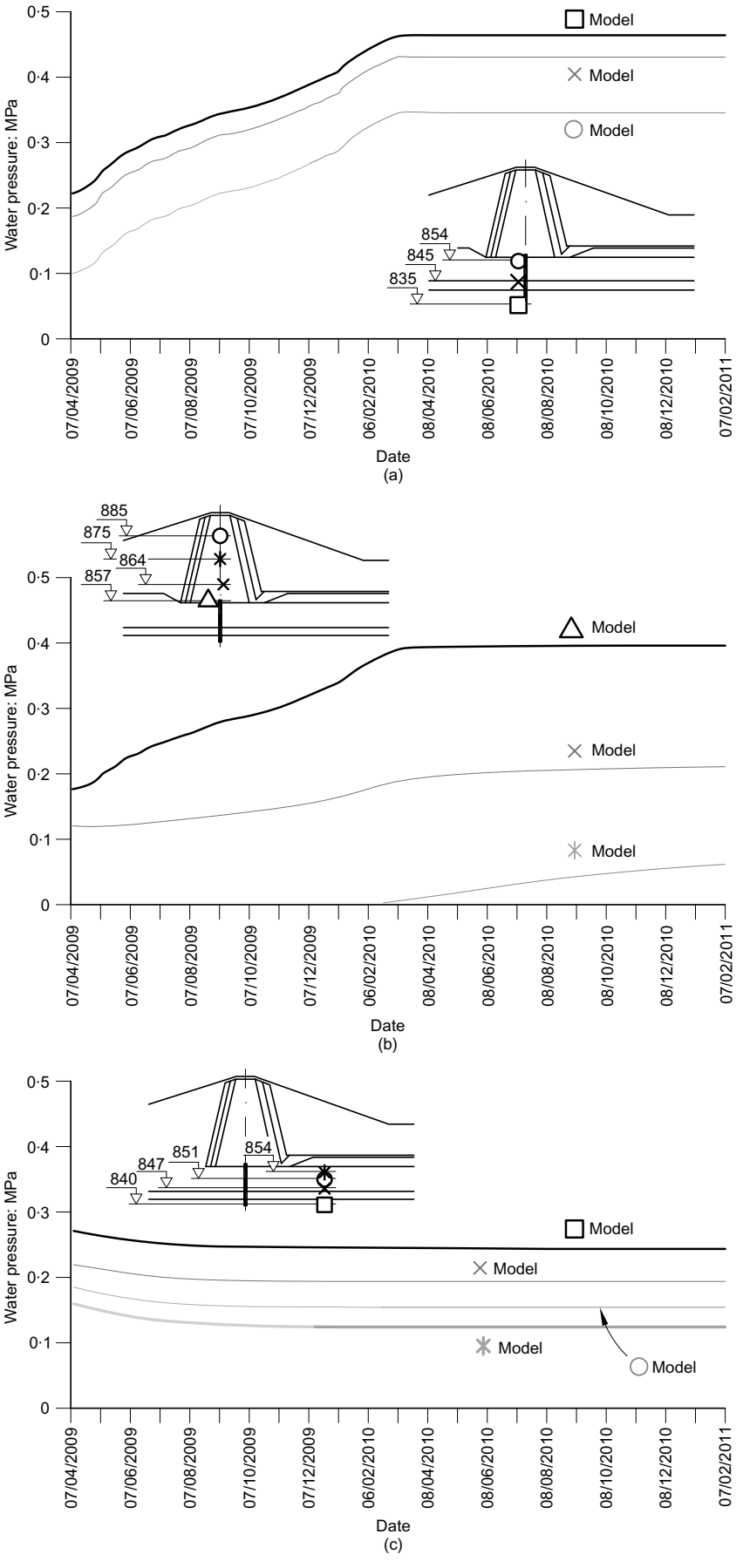

Fig. 28. Calculated pore-water pressures in the locations indicated during dam impoundment: (a) foundation soils, under the core; (b) clay core; (c) foundation soils, downstream

the dam during impounding and some predictions of stress, settlements and pore pressure developments at the position of installed instruments have been given in the paper in order that they could be compared in the future with actual measurements.

REFERENCES

Alonso, E. E., Gens, A. & Josa, A. (1990). A constitutive model for partially saturated soil. *Géotechnique* **40**, No. 3, 405–430, **doi**: 10.1680/geot.1990.40.3.405.

Alonso, E. E., Olivella, S. & Pinyol, N. M. (2005). A review of Beliche Dam. *Géotechnique* **55**, No. 4, 267–285, **doi**: 10.1680/geot.2005.55.4.267.

Chávez, C. (2004). *Estudio del comportamiento triaxial de materiales granulares de tamaño medio con énfasis en la influencia de la succión*. PhD thesis, Universitat Politècnica de Catalunya, Barcelona, Spain.

Chávez, C. & Alonso, E. E. (2003). A constitutive model for crushed granular aggregates which includes suction effects. *Soils Found*. **43**, No. 4, 215–227.

Chávez, C., Romero, E. & Alonso, E. E. (2009). A rockfill triaxial cell with suction control. *Geotech. Testing J.* **32**, No. 3, 219–231.

Coussy, O. (1995). *Mechanics of porous continua*. Chichester, UK: Wiley.

Daehn, W. W. (1985). Behaviour of a rolled earth dam constructed on a compressible foundation. *Proc. 5éme Congrès des Grands Barrages, Paris* **Q18**, R7, 171–191.

DIT-UPC (2002). *Code_Bright. A 3-D program for thermo-hydro-mechanical.analysis in geological media. User's guide*. Barcelona, Spain: Centro Internacional de Métodos Numéricos en Ingeniería (CIMNE).

Gens, A., Sanchez, M., Guimaraes, LdN. *et al.* (2009). A full-scale in situ heating test for high-level nuclear waste disposal: observations, analysis and interpretation. *Géotechnique* **59**, No. 4, 377–399, **doi**: 10.1680/geot.2009.59.4.377.

Oldecop, L. (2000). *Compresibilidad de escolleras. Influencia de la humedad*. PhD thesis, Universitat Politècnica de Catalunya, Barcelona.

Oldecop, L. & Alonso, E. E. (2001). A model for rockfill compressibility. *Géotechnique* **51**, No. 2, 127–139, **doi**: 10.1680/geot.2001.51.2.127.

Oldecop, L. & Alonso, E. E. (2003). Suction effects on rockfill compressibility. *Géotechnique* **53**, No. 2, 289–292, **doi**: 10.1680/geot.2003.53.2.289.

Oldecop, L. & Alonso, E. E. (2007). Theoretical investigation on the time dependent behaviour of rockfill. *Géotechnique* **57**, No. 2, 289–301, **doi**: 10.1680/geot.2007.57.2.289.

Olivella, S. & Alonso, E. E. (2008). Gas flow through clay barriers. *Géotechnique* **58**, No. 3, 157–176, **doi**: 10.1680/geot.2008.58.3.157.

Olivella, S., Carrera, J., Gens, A. & Alonso, E. E. (1994). Non-isothermal multiphase flow of brine and gas through saline media. *Transp. Porous Media* **15**, No. 3, 271–293.

Olivella, S., Gens, A., Carrera, J. & Alonso, E. E. (1996). Numerical formulation for simulator (CODE_BRIGHT) for coupled analysis of saline media. *Engng Comput*. **13**, No. 7, 87–112.

Ramírez, J. L., Soriano, A. & Serrano, C. H. (1991). Design and construction of Barbate dam. *Proc. 17th ICOLD, Vienna, Austria* **Q67**, R8, 129–163.

Rizzoli, J. L. (1991). Observations du comportement de fondations compressibles: barrages des retenues Seine, Aube et dique de Lazer. *Proc. 17th ICOLD, Vienna, Austria* **Q66**, R8, 129–163.

Tellería, J. & Gómez Laa, G. (1991). Arbon dam: A didactic experience about problems of a dam built on a deformable foundation. *Proc. 17th ICOLD, Vienna, Austria* **Q66**, R9, 135–156.

Torner, V. & Novosad, S. (1991). The effect of difficult foundation conditions on the conceptual solution and construction of the Slezská Harte dam. *Proc. 17th ICOLD, Vienna, Austria* **Q66**, R40, 719–730.

Trkeshdooz, R., Nafissiazar, F. & Rastegari, Y. (1991). Effects of foundation conditions on the design of Taleghan embankment dam. *Proc. 17th ICOLD, Vienna, Austria* **Q66**, R75, 1415–1488.

van Genuchten, M. T. (1980). A closed-form equation for predicting the hydraulic conductivity of unsaturated soils. *Soil Sci. Soc. Am. J.* **44**, 892–898.